

# **A solution to the high bias in estimates of carbon held in tropical forest above-ground biomass**

**H. Arellano-P.<sup>1,2</sup> and J. O. Rangel-Ch.<sup>1</sup>**

[1]{Grupo de Investigación en Biodiversidad y Conservación, Instituto de Ciencias Naturales, Universidad Nacional de Colombia, P.O. Box 7495, Bogotá D. C., Colombia}

[2]{Compensation International Progress S.A., P.O. Box 260161, Bogotá D. C., Colombia}

Correspondence to: H. Arellano-P ([harellano@unal.edu.co](mailto:harellano@unal.edu.co))

## **Abstract**

**Non-destructive methods were used to estimate the volume, aerial biomass and amount of carbon stored by individuals of different plant species, communities, vegetation types and coverage based on using elemental information capture, three-dimensional architecture and recurrent neural networks. This methodology accurately captures the diversity of plant forms present in plots or relevés. The calculation of stored carbon in a vegetation type is a result from half the estimates of the biomass of sampled individuals in significant plots by the use of allometric formulas. The most complete formulas incorporate the diameter, height and specific gravity of trees but do not consider the variation in carbon stored in different organs or different species as well as exclude information on the wide variety of architectures present in different plant communities. To develop an allometric model, many individuals of different species must be sacrificed for the identification processes, validation and error minimization. It is common to find cutting-edge studies in which logging is**

**encouraged to improve estimates of carbon. In this study, we replace this destructive methodology and provide an important contribution to quantifying global aboveground carbon. We have demonstrated with our methodology that carbon content in forest above-ground biomass in the pantropic could rise to 723.97 Pg C. This would involve the reassessment of many climatic and ecological models in order to move towards a better understanding of the adverse effects of climate change.**

## **Introduction**

The large uncertainty in estimates of biomass and carbon content in tropical forests (1, 2) is of great concern to the scientific community. Governmental and non-governmental entities responsible for developing and implementing policies and mechanisms to assist in the mitigation of climate change, such as Reducing Emissions from Deforestation and forest Degradation (REDD+), are also stakeholders. To estimate the losses or gains of multi-temporal carbon for a given area, two key inputs are necessary: thematic mapping coverage for at least two time periods, which is used in the analysis of deforestation, degradation and changes in land use; and calibrated results of biomass and carbon estimates for different types of vegetation obtained using different methods. The most commonly used method worldwide for the estimation of forest biomass is the sum of the biomasses of the sampled individuals, which is determined with an allometric model. For the development of a model of this type, the sacrifice of many individuals from various species (2, 3, 4) is necessary for the process of determination, validation and error minimization. The collection of information on the weights of between 2,410 and 4,004 trees, which were cut down and segmented, was required for the generation of the allometric equations typically used in the tropics (2, 4, 5). The biomass results obtained with the traditional method have an

undetermined bias (4) towards individuals with a diameter at breast height (DBH) of less than 5 cm and greater than 156 cm (4) to 212 cm (2). Such results often involve misinterpretations of the statistical coefficient of determination ( $r^2$ ) (6), generating a false impression of the reliability of the models. This situation was also evident for other proposed equations (3, 5, 6) for which similar trends and results were found, attributed mainly to the mathematical structures that they share. In many cases, only the constants were different between equations. For these reasons, we believe that using the traditional methodology to expand current knowledge as proposed in the principal research in the field (1, 2, 3) will have a high economic cost, increase unwanted deforestation and intervention in pursuit of knowledge, incorporate errors resulting from the cutting and weighing methods into the resultant equations, and require a time frame greater than 50 years to produce an information base adequate to increase the accuracy of the results (4). The lack of data from pantropical studies and the use of estimates derived from the compilation and synthesis of existing information only for the Amazon, which are based on sampling plots that represent only one-millionth of its area (7), contribute to the insufficient information that directly affects our understanding of climate change, deforestation, ecosystem degradation, mitigation mechanisms and thus the future of life on the planet. Moreover, the importance of carbon held in biomass is recognized by the scientific community; however, because of the diversity, floristic composition, tissues and organs examined, stand age, population density of each stratum and other variables within plant communities, differences in the carbon percentage held in biomass range between 43% and 58% of the total biomass (8). Dividing the total biomass by 50% in calculating carbon reserves is promoted by the Intergovernmental Panel on Climate Change (IPCC) (9).

To address this concern, we wondered if there was the possibility of developing an alternative that would answer to these multiple disadvantages, whereby we spent more than four years collecting information on different vegetation types established in a meso-climate tropical gradient in the Colombian Caribbean and developed a new, non-destructive methodology using three-dimensional modelling based on the species present in typical plots, their organs and species- and organ-specific carbon storage data derived from small tissue samples. This information, together with knowledge of these species' regional distribution, enabled us to replace the use of allometric equations. In other words we introduce a new method, which is based on 3D modeling to estimate the volume by considering different organs of the multiples individuals from different plots. With this new methodology, we were able to estimate the amount of carbon held in the forest aerial mass with surprising accuracy (error values were between 1.79% and 4.03%), which we believe renders obsolete the destructive techniques promoted in the past as a solution to decreasing the error in estimates of the distribution of biomass and carbon in the tropical region (2, 3). With our results we calibrate the pantropical carbon estimates to date, which result allowing us to compare our method with two previously reported estimates of the contribution of forest aerial mass to the total pantropical carbon. Tropical forests are also both biodiverse and morpho-diverse, further complicating estimates of above-ground biomass.

## **Results**

In an area of 3,425,083 ha in southern and north-western Cordoba in the Colombian Caribbean and delimited by UTM coordinates (datum WGS 84 zone 18 N 78-72 W) 1,030,572 North, 835,192 South, 348,788 West and 529,688 East. We analyzed structural information from 6,141 individuals of 938 species in 112 plots and collected from 27 forest

types along an altitudinal gradient from 0 to 1,839 m. With this information, we were able to differentiate the floristic composition characteristics of 27 high shrubs resulting from the degradation of forests, a grassland interspersed with areas of human intervention, and five combinations of coverages where agricultural use predominates. Among all of the coverages, for carbon sampling, we chose four representative vegetation regions belonging to several forests that were dominated and characterized by *Jacaranda copaia* & *Pouteria multiflora*; *Protium aracouchini* & *Virola elongata*; *Trichilia hirta* & *Schizolobium parahyba* and *Acalypha* sp. & *Guazuma ulmifolia* (10, 11), set in a tropical climate gradient from a super-humid climate with rainfall between 2,200 and 3,000 mm per year to a semi-humid climate with rainfall between 1,000 and 1,400 mm per year. It is noteworthy that because of their floristic composition, these vegetation types contain the information necessary for inferring the characteristics of other vegetation assemblages. We present the details of the spatial distribution of all the characterized vegetation types in (12).

The estimated summary volume and biomass values per individual in the plots are observed in Table 1. The total values are noticed in Supplementary tables S1-S3.

### **Results biomass comparison with allometric methodologies**

After the biomass determination using a three-dimensional modelling of the species and their relation to tissues density (see methods), we compared the results with a more accurate and traditional methodology based on the application of allometric equations for the different analyzed organs (13), where equations are used for the stem, large branches and twigs. The only important comparative example of this type, shows that the contrast of equality hypothesis of covariance for the X matrix (DBH, height, biomass of the stem and the main branches, secondary branches or twigs, leaf biomass and total biomass three-dimensional modelling) and Y matrix (the same structural variables as X and the biomass of

the organs estimated with allometric equations) (13) was rejected in all cases. The rejection of the hypotheses in these cases indicates large differences between the contrasting methods (Table 2).

With this we demonstrated that this bias is present without distinction over the full range of DBH values because the formulas are unable to incorporate information on the heterogeneity of the forms of individuals.

However, the methodology that uses allometric equations, which is widely used to estimate this variable in both tropical forests established in wet and dry weather, was published in (4). Its implementation was highlighted by (14) and (15) by including trends from nine other similar methodologies. These equations, present not only the highest correlations between the resulting data, but also the feature of being able to integrate records from the wood density. It is noteworthy that (16), published several equations which once applied to the variables DBH, height and wood density, generate a greater biomass estimation, although describing the same mathematical behavior recorded by the equations of (4).

In Figure 1 comparison of the estimated biomass can be observed for the established forests in the gradient from super humid to humid climates and dominated by the associations *Jacaranda copaia* & *Pouteria multiflora*; *Protium aracouchini* & *Virola elongate* and *Trichilia hirta* & *Schizolobium parahyba* using the methodology proposed in this study and the traditional methodology published by (5) for the different organs studied in the DBH range from 1 to 20 cm. As seen in this range, all biomass' estimates found in this study are around (not similar) the estimated records of the allometric equations of (5). It is noted that due to the three-dimensional method, it is possible to incorporate the high structural variability present in the sampled regions and the biomass of the individuals is estimated with greater accuracy. Overall, for the results obtained by the traditional methodology, both for the

estimation of organs (5, 13) and the whole individual (4), the trend of homogenization of the records and the removal of the proper extreme values of specific species or of characteristics that favor or not the growth of individuals (which are triggered by local environmental conditions and which should be reflected by the biomass records), is observed. Similar cases to the ones previously exposed are presented for the comparative records of secondary branches (twigs), the leaves and the biomass records for the whole individual (Figure 1-2, 3 and 4-). Supplementary Table S2a, the final results are observed regarding the biomass estimation for the modelled individuals from the forest communities established on humid to super-humid climates in the DBH range of 0-20 cm. Differences between these results are shown as well as those found through for (5) equations.

In Figure 2, same comparison in the DBH range between 20 and 200 cm are presented. At this point, it is worth mentioning that since the biomass estimation is linked to the cubic increase of the doubling of the dimensions, the differences between the methods are also increased when the DBH is increased. It should be noted that in the estimated biomass records for the leaf component, larger data dispersions are presented, relative to the estimated value by allometry. In (5) recognized many deficiencies in the method, situation that is represented by the concentration of the records obtained from this method in the center of the figure (Figure 2 -3). For the records of final above-ground biomass (belonging to the sum of all components), a similar behavior to the one of the main branches records is presented (main stem and branches), which shows once again the great contribution of this component to the results. Supplementary Table S2b, shows the final values for the biomass estimation for this DBH range of 20-200 cm. For the types of vegetation established in semi-humid climates the comparisons can be noticed in the Supplementary note S1.

When exploring the basic structural data (DBH, height and density) in the most common allometric equations (14), high correlations between the evaluated results of nine equations are observed, situation that is evidenced by the massive use of these equations. For this reason the equations of (4) are chosen as the model summarizing the behavior thereof. Following this indication, these equations are compared with the records of biomass estimated by the three-dimensional modelling methodology. By comparing the records found by the equations of (4) and (5), it can be observed that the first ones are more dispersed in smaller DBH intervals and, the latter, in larger DBH intervals, in Supplementary note S1 this results can be observed.

Based on the results of the spatial distribution of the vegetation types and the covers, that where generated from the application of the CCA-Fuzzy Land Cover method and published in 12, we estimated the results of the carbon estimation per hectare. To achieve this we extrapolated and calibrated by density analysis and artificial neural network back-propagation for the surface sampled (Supplementary note S2), showed that a total of 9,559.64 Mg C (implying an overall average of 177.03 Mg C ha<sup>-1</sup>) was recorded for 54 vegetation types with the implementation of the methodology proposed in this study.

Regional estimates of carbon with the traditional methodology showed a value of 3,316.08 Mg C, or 61.41 Mg C ha<sup>-1</sup>. The difference between the two methods was 6,243.56 Mg C for the 54 vegetation types studied, i.e., a difference of 115.62 Mg C ha<sup>-1</sup>, which corresponds to 65.3% of the result from the non-destructive methodologies. For primary tropical forests in super-humid climates in sites associated with water bodies, little to no intervention, and dominated and characterized by *Macaranga ischnocalyx* & *Peltogyne purpurea*, the higher carbon content per hectare was 523.4 Mg C (traditional methodology, 290.63 Mg C ha<sup>-1</sup>; difference 232.77 Mg C ha<sup>-1</sup>, or 44.47%). For primary tropical forests present in super-

humid climates, with low to medium intervention, and dominated and characterized by *Jacaranda copaia* & *Pouteria multiflora*, the higher carbon content per hectare was 437.25 Mg C ha<sup>-1</sup> (traditional methodology, 196.01 Mg C ha<sup>-1</sup>; difference 241.24 Mg C ha<sup>-1</sup>, or 55.17%). For primary tropical forests in super-humid climates in sites with little or no flooding, little to no intervention, and dominated and characterized by *Prestoea decurrens* & *Trichilia poeppigii*, the higher carbon content per hectare was 428.62 Mg C ha<sup>-1</sup> (traditional methodology, 267.71 Mg C ha<sup>-1</sup>; difference, 160.91 Mg C ha<sup>-1</sup>, or 37.54%). Given that the consolidation of the final results per hectare (Supplementary note S2) represents information comparable to nearly the entire carbon storage gradient reported in the pantropical map published in 2012 (1), we used the information from the tree height distribution map (17) to generate a calibration model for the artificial neural network and create the calibrated carbon pantropical map (for the period 2007-2008; Figure 3, extended data). It is noteworthy that the differences reported by (18) for the carbon storage pantropical map 2012 (1) do not arise from regional variations in wood density and its relation to the height and DBH but, rather, a combination of the scale of comparison, the objects compared, methods of regionalization and mainly, as explained here, the allometric models used.

The artificial neural network training values for the south-western region of the Colombian Caribbean were between the minimum and maximum limits: i.e., 0 and 190 Mg C ha<sup>-1</sup> and 0 and 38 m in the variable height of individuals as input from (1) and (17), respectively. The values in the response range from 0 to 523 Mg C ha<sup>-1</sup> were based on data derived from the carbon stored to the region estimated in this contribution. The results of the processes of training, testing and validation had correlation coefficients  $R = 0.996$ ,  $0.997$  and  $0.988$ , respectively (i.e.,  $R = 0.995$  overall), which legitimized this procedure (Figure 4). Thus, it

was determined that the maximum value of carbon storage in aboveground biomass in the tropics, is approximately  $605 \text{ Mg C ha}^{-1}$  ( $251.5 \text{ Mg C ha}^{-1}$ ) (1). Based on this calibration model estimates that the carbon stored in the pantropical region would be around of  $723.97 \text{ Pg C}$  (Figure 3), which implies that estimates of (1) and (3) represent only the 31.59% ( $228.7 \text{ Pg C}$ ) and 39.38% ( $285.1 \text{ Pg C}$ ) respectively, compared to our methodology. The greatest differences in the carbon content between the carbon map (1), generated previously, which is the most accurate map published to date and that generated in the present study can be attributed to the fact that, high-precision Light Detection and Ranging (LIDAR) data used in the first map (1) were calibrated with carbon values per unit area, which were derived from half the estimates of the biomass of sampled individuals by the use of allometric formulas. The most complete formulas (2, 4, 6, 19) incorporate the diameter, height and wood density of trees but do not consider the variation in carbon stored in different organs or different species as well as exclude information on the wide variety of architectures present in different vegetation communities.

In Table 3, a comparison among the various arbitrary intervals shows the carbon storage per hectare in the pantropical region of the world (excluding the Australian tropical region). It is worth noting that these values are the summations of records calibrated from carbon per pixel from the matrix arrangement of the maps. In addition, the sum of the data from the pantropical map published in 2012 (1) and those available nationally in (20) does not correspond to the final value of  $228.7 \text{ Pg C}$  reported in (1) but, instead, to  $227.42 \text{ Pg C}$  because the information provided in this link was modified to provide information at the national level. Despite this adjustment, comparisons, trends and differences are valid for the analyzed regions. As expected, a huge difference (between  $-405.80\%$  and  $100\%$ ) in all of the classes evaluated was observed in this redistribution of carbon content values for the

pantropic regions. Three new classes of between 300 and 605 Mg C ha<sup>-1</sup> were generated. 583.55 Pg C are sequestered, meaning it is slightly more than 80% of the pantropical total. The largest percentage difference was found for the regions with a content of between one and 50 Mg C ha<sup>-1</sup> that only stores 8.83 Pg C (Pg C 44.68, -405.8%) (1). Thus, we estimated that a biomass near 382.85 Pg C (117.7 Pg C, 30.74%) (1) is stored in America, followed by Africa with 175.77 Pg C (64.5 Pg C, 36.69%) (3) and Asia-Oceania with 165.35 Pg C (46.5 Pg C, 28.12%) (1). In table 4, countries with higher carbon stocks are observed.

## Discussion

With these results we could conclude that the voxelisation method is much more accurate, even more than the volume calculation method by water displacement, due to the fact that the sample (the whole individual) loses its integrity when cut in multiple pieces and a tendency of volume diminution is presented from handling resolutions inferior to one cubic centimeter (more precise).

The wide range of estimates of carbon reserves, together with the factors outlined above, indicates that data from remote high-precision sensing methodology (LIDAR), which is negatively affected by the need of calibration by using as input information field data, which is typically derived from the traditional destructive methodologies described above. Moreover, we note with concern that the results generated to date are based on a lack of vegetation types growing in different soil types and do not count for the varied pantropical geography. Ignoring the floristic composition and vegetation ensembles in these thematic maps, regardless of the quality and resolution of the inputs used in their construction results in unpredictable increases in the error in the final estimates. Some authors use generic logarithmic equations to estimate the error in the underestimation of biomass stocks to be

between 0% and 40% (19) for certain regions, whereas according to our results, the error distribution associated with the traditional method may vary between 36% and 96% (Supplementary note S2).

Finally, one might believe that the impact of the deforestation and degradation of tropical forests, climate change, the greenhouse effect and the total percentage that this transformation of land use contributes to the phenomenon of global warming is more serious than that reported to date, but new evidence and climate models to test this possibility are essential; thus, these results should be analyzed with caution. A review of contributions such as those in (21), the consolidation of actual values on deforestation in the tropics and a precise value for the atmospheric carbon contribution are required to strengthen the mechanisms and efforts to mitigate the adverse effects of climate change and to provide the necessary security to carbon markets, which are one of the main methods of mitigation. The methodology presented here is useful for improving knowledge on the distribution of biomass and carbon on the planet, and this methodology is immediate applicable to projects that characterize and evaluate the environmental services of biodiversity, such as carbon storage for REDD+ projects.

## **Methods**

## **Synthesis**

An examination of the traditional methodologies (2, 3, 4, 5) that have been applied for over half a century (22), for the quantification of biomass and therefore of carbon in tropical regions, revealed that several processes could be replaced with the help of technological tools. It was inconceivable to us that to calculate the weight of a tree, the tree would have to be cut down, because techniques to calculate the precise volume of trees by three-

dimensional modelling of their organs and estimating their weight exist, relating the values obtained to their respective densities. Because of the automobile industry, aeronautics, video gaming and cinematography, which have invested considerable sums of money in the development of increasingly sophisticated algorithms to capture shapes, one can model any object with high metric accuracy and can even simulate actual physical conditions that affect the object. The use of these technologies has been widely accepted in various scientific disciplines, such as the design small and large mechanical parts and the planning of complicated medical operations. Thus, individual plants sampled in the south-western Colombian Caribbean were modelled with the combined use of drawings, photographs, Bezier curves, NURBS (Non - Uniform Rational B -Spline) and the latest surface algorithms.

Because they contain advanced organic modelling and dimensioning tools, the capacity to generate different levels of surface quality and the ability to recreate trees with great speed, routines available in commercial software packages (SpeedTree studio 6.1.1 and Xfrog 4.5 for Maya 2009) were used. The process consists of combining basic structural information (DBH, height and coverage) with data from statistical counts, illustrations and field photography, such as the levels of branching, number of branches and branch thickness and adjusted distance metrics to generate a matrix model XYZ in normed vector space  $\mathbf{R}^3$ . Modelling leaves was also performed. To relate the carbon records for each of the sampled plant organs, the final branching three-dimensional model was separated into a group that contained thick stems and another that contained young branches and their bark. Volume was calculated by numerical integration (23, 24) and the voxelisation (25, 26) of 221 individuals represented by tridimensional models belonging to 127 species. The DBH of the modelled individuals has a length of 195 cm, and a DBH ranging from 1.83 cm to 195

cm. The corrected height of the evaluated models showed 45.19 meters in length; the lower and upper limit were 2.01 meters and 47.92 meters, respectively. Measurement comparisons in the different software packages with 3D metric manipulation capabilities (Maya, Surface and Rhino3d, among others), show the correct bounding of the models. According to a preliminary DBH classification, 174 individuals were recorded in the range of 1.83 cm to 50 cm. Of these elements, more than half do not reach 30 cm of DBH. Between 50 and 100 cm, 32 individuals were modelled, of which more than half do not exceed 70 cm in diameter. Between 100 and 150 cm, and between 150 and 197 cm, five and four individuals were modelled, respectively.

The biomass of the individuals was obtained by summing information related to the wet and dry density of the sampled stems from the primary and secondary branches, bark and leaves. Following this process, we compared the biomass with the carbon content of the samples at specific and intraspecific levels considering that the carbon concentration in the organs is variable (27, 28, 29). In species from the region, a carbon concentration representing between 41.11% and 49.99% of the total biomass was recorded. Part of this analysis was published in (14). After recording the total carbon information for the individuals, we classified them by architecture (30) to incorporate the morphological heterogeneity of the vegetation. Artificial neural network calibration models with training matrices for different intervals of DBH were built, which also combined the type of architecture, DBH records, height and specific gravity of the wood. The response variable was the amount of carbon in the biomass found using the three-dimensional modelling-based methodology. Therefore, the storage element was satisfactorily calibrated in 5,920 individuals whose only known information was their typical structure. In total, information from 6,141 individuals was consolidated. The overall correlation coefficients between

processes ranged from  $R = 0.73$  to  $0.97$  and were lower for less frequent architectures, as expected. We then calculated the carbon stored in different vegetation types and analyzed and compared the carbon values with the results obtained with allometric equations (4, 13) (Figure 5). To calibrate the density of individuals per unit area and extend our observations to surfaces greater than one hectare, we generated an analysis of floristic similarities by main coordinates (MDS) of Sokal and Michener's distances and structural analysis using canonical populations (MANOVA) for the dominant species of tree belonging to different strata of vegetation types established in Colombia, Panama and Costa Rica (31, 32). Then, we produced a regional estimate of the total carbon content relating the values obtained with the map of vegetation types for the south-west Colombian Caribbean (33). Finally, to calibrate the pantropical carbon, multiple statistical tests were performed to determine the use of training variables, elevation, annual amount of precipitation, monthly average temperature, pantropical carbon (1) and tree height (17). The best results were obtained with the last two variables.

### **Determination of biomass using three-dimensional modelling of the species and their relation to tissues density**

For better understanding of the tridimensional processes performed on the normed vector space  $R^3$ , we need to understand the basic geometry of three-dimensional computational objects. A classic three-dimensional object, comprises three distinct elements: the vertices with  $XYZ$  coordinates, which limit geometric shapes in the two-dimensional normed vector space  $R^3$  (Euclidean space  $R^3$ ); faces, corresponding to the area bounded by the vertices and are represented as a matrix-consecutive number that identifies each of the two-dimensional geometric shapes; and the normals of the faces, which are vectors with  $XYZ$  coordinates, perpendicular to each of the sides, usually of unitary magnitude, that allow the

identification of the surface direction, in addition to other geometrical properties. In other words, they enable in this case, the identification of the convex faces in the model. In Figure 6 the building process of three-dimensional model, can be observed.

In the precise computational volume calculation of three-dimensional objects with complex surfaces, there are two methods discussed in the literature: the numerical integration method, based on input from (23), and the object voxelisation based on (25). For the correct calculation of the volume of individuals by the method of numerical integration (vector method), it is necessary to obtain a homogeneous and topologically closed triangular mesh. In the case of the voxelisation method (3D raster method), it is only necessary a closed mesh, independent from the arrangement of vertices in triangles, squares, or other two-dimensional geometric configurations in the normed vector space  $R^3$ . It is worth noting that in the latter method, the homogeneity of the mesh is not necessary.

In the numerical integration method developed by (23), in addition to the volume calculation over the volume on rigid body models composed of uniform density polyhedra, the mass center, momentum and inertia tensors, are calculated with an algorithm that minimizes the error caused by probable misalignments of the polyhedral faces. In general, the method consists of three steps in which volume integrals are simplified, applying the theorems of divergence, projection and Green (23). In this contribution, the adaptation of MATLAB 2011b was used (developed by Andrew Gosline of the C code programmed by 23), where part of the code was modified to increase the computation speed and generate the batch file process. The method also allows the possibility of correcting the records of the individuals height (in several cases, by keeping the girth at breast height -GBH- record intact and comparing it with the scaled records graphics, such measurement is corrected), capture information about the growth angles, leaves insertion angles, branch density,

density of projected shadows at different times of the day, calculate the mass center, mass momentum, inertia tensor, surface, actual coverage, volume and the effect of natural and anthropogenic disturbance in the growth of trees.

Voxelisation methods are intended to achieve a continuous geometrical representation by a set of voxels to exemplify a real object in the best possible way (25). Voxels, as their two-dimensional counterparts, the pixels, can be manipulated by choosing the desired cubic unit to define the overall resolution of the object. In this sense, the representation of trees by voxels with current technology, could be done in micrometer, millimeter or centimeter scales. It should be emphasized that the choice of one or the other, depends mainly on the constraints imposed by the hardware configuration used.

One cubic centimeter was selected as unit for individuals with less than 15 m height; 1.95 cm<sup>3</sup> (half inch cubed), for some individuals between 15 and 20 meters, and covers with sides lower than 10 m; 8 cm<sup>3</sup>, for individuals with heights between 15 and 30 meters and 15.62 cm<sup>3</sup> (cubic inch), for individuals over 30 m. The choice of these units is mainly due to the fact that the voxelisation method generates a logic matrix that emulates in small compartments, the space that occupies a determined object and its complement, to fill a hexahedron. This means, that in the centimeter scale, the representation of structures that fit a cube of 15 m side, generates about 3,375,000,000 of data, situation in which, by doubling the height, the amount of memory space required (RAM) is cubed and so is the time required to perform the same calculation by the computer. To represent all the trees into small units, excessive time will be required as well as the generation of a new computational code to split large files or the implementation of a computer farm for its calculation. On the contrary, the choice of the largest unit (cubic inch), to analyze all modelled trees, would adequately represent large volumes and it would even compensate

the calculus of unmodeled structures inferior to one square inch in cross-sectional area. However, for individuals with lower heights, the error would increase in inverse proportion to its height. For this reason, all individuals were voxelized with logical matrices that did not exceed 3,375,000,000 of data and correspond to the selection of the above cubic units. Correction factors were also incorporated, calculated by comparing similar volumes in different cubic units. This, for models in which individuals are represented by a unit different than the cubic centimeter (cubic feet, cubic inch). Among voxelisation models, conversion scanning, the paired count, distance projections and light ray simulation stand out. In this contribution, the ray tracing simulation was used, by which the intersections between simulated light beam (fired orthogonally to the modelled object ) are found for each of the X, Y and Z edges and the sides, in the normed space  $R^3$ . The mathematical explanation that underlies the implementation of the method can be consulted in (34) and (35). It is important to highlight, that the length of each axis corresponds to the actual dimensions of the object in the unit of the chosen measure. These dimensions are found by the difference between the maximum and minimum (limits) of the coordinates of the vectorial model. This process, considers as filled and true space (existence of matter in space  $R^3$  normed), the regions present between an odd intersection and the following simulated light beam. In other words, this calculation involves simulating through geometric equations, the path of a light ray, which intersects a vector object (vertexes, normals and faces) from a light source to a point in the image plane or screen. To increase the computation speed, the process is reversed, and any calculation that does not generate a solution of the image plane is deleted. The logical values (true or false) along the path of each simulated rays for each voxel projected on the screen, generate a three-dimensional logic matrix, containing information on the existence of the object in the space  $R^3$ . It is

worth mentioning, that these records do not contain positions in  $X, Y, Z$  space, but its position is deduced by the place occupied by a real value in the matrix and voxel size (25). Thus, it is possible to logically represent complex objects and calculate their volume using the continuous sums of the areas evaluated as true in the resultant three-dimensional logic matrix. It's important to highlight that actually we are working to improve the modeling through the relation between our models and the architecture data captured by a LIDAR mobile. In Figures 7 and 8, the most important characteristics of a homogeneous triangle mesh are observed, necessary for the estimation process by numerical integration. The three-dimensional modelling besides, the possibility of correcting the records of the height of individuals (in several cases, by keeping the girth at breast height (GBH) record intact and comparing it with the scaled graphic records, such measurement is corrected), the method captures information about the growth angles, leaf insertion angles, branch density, density of projected shadows at different times of the day, calculate the mass center, mass momentum, inertia tensor, surface, actual coverage, volume and the effect of natural and anthropogenic disturbance in the growth of trees. In Figure 9, the result of the representation of two of the constructed trees by the voxelisation process can be observed. To develop this process, part of the (26) code was modified to increase the computational speed, calculate the dimensions of the modelled trees, calculate the volume and generate the process for files batches. It is important to emphasize that the measures enclosing the models were evaluated in different software (Maya, Surface and Rhino3D) in order to find inconsistencies.

The palm stems were included in the analysis as deformed cylinders. For species that retain part of the leaf sheaths, these structures were estimated within the leaf modelling. It is important to mention that in this work, the first level of branching was considered as the

one coming from the trunk or stem (which collectively form the main branches). The higher levels: three, four, five and six, represent the secondary branches, where the higher ones are the youngest and thinner.

After the detailed estimation and calibration of the architecture volume of the corm without leaves or roots, we proceeded to estimate the branch volume from the upper levels to the third, following the same methodological route. The previous procedure, in order to differentiate the volumes of the bodies, primarily separated by thickness and therefore by age. We proceeded to estimate the volume (volume of a right prism trapezoidal base) by the ratio of the total area of the individual (estimated regardless existing transverse regions), and the surface of the branches with the measured depths of their respective bark. Equation 1 was used for this, depending on the thickness of the bark and the surface of the examined organs. It is worth mentioning, that it is possible to detail the model's surface model according to the bark morphological characteristics. This could be achieved by incorporating information about its texture in normal textured maps (normal maps), deformation (bump maps) or generating periodic noise (noise), as applicable. However, due to the required computational load, this process was omitted for the job. Furthermore, some structures present in the bark such as decorations, rings or spines were modelled according to the increase that these structures generated in the computer algorithms. When this was positive, it was decided to multiply or divide the bark volume with a correction factor estimated in a model or segment model with less stored information. The size of the file depends on the complexity of the modelled structures, the format used, and the density of the triangles or squares mesh and on the generalization processes. The STL (stereo lithography) format was chosen because it stores the topological structure effectively as a text file (vertexes, normals and faces indexing). For this reason small file sizes (about 60

Megs disk) can store a big amount of information. With a file of this size, 2,630,322 normals and 292,258 normal individual faces of *Cedrela odorata* 19.51 cm DBH and 10.35 m high, can be represented by means of 2,630,322 vertexes. A more complex individual such as *Caryocar amygdaliferum* of 123.75 cm DBH and 41.71 m, height requires about 300 Megs disk (13,239,287 vertexes).

**Equation 1.** The volume of  $V_c$  bark is estimated for main and secondary branches, based on the initial and final bark thickness,  $C_i$  and  $C_f$  and the surface of organs  $A$ , (volume of a straight prism with trapezoidal base).

$$V_c = \left( \frac{(C_i + C_f)(A^{1/2})}{2} \right) A^{1/2}$$

With the volumes found by numerical integration and voxelisation methods, we proceeded to the calibration of the models, especially those that were performed by the voxelisation technique with different units than the cubic centimeter. In order to obtain records of the individual moisturized biomass, the stem volume and main branches, high level branches and bark, were multiplied by their respective green density registers (14). Through the existing relationship between weight records among the wet and dry sampled material, biomass and water content of the individual were found. With the biomass registration of each of the organs tested, we proceeded to the carbon reserves' punctual estimation. It is worth mentioning, that the analysis and discussion about carbon reserves at an intra and inter specific level (organs and species), as well as the consequences of carrying out this procedure are discussed in (14) and (15). It is important to highlight that the virtue of the numerical integration and voxelisation methods, were compared with calibrated values resulting from ROC methodology.

## Leaves Treatment Methodology

Volume estimates, related to the leaves contribution of biomass and carbon, was approached by a different treatment which can be summarized by three steps: the statistical count of the number of leaves in the different branches, the detailed area estimation and the relationship of the latter with the layer thickness. It is worth mentioning, that in all cases the petiole was included within the calculations.

In estimating the number of leaves present in a particular individual, the SpeedTree studio 6.1.1 software was used, which incorporates the minimum and maximum organ counts made in each branch level. The incorporation of a motor generating pseudorandom numbers within these limits stands out. As a result, a matrix with information of the leaf number per branching level is obtained, which is multiplied with the most frequent volume estimation that acquires a leaf in that level. To estimate the layer area, the data capture through photography or drawing ink on white paper of the silhouette of the leaves collected in the field, is firstly needed. Most of this work (collection, silhouettes hand drawing and scanning) was performed by (15). (Other part was developed by 36). With digital information in raster format, mosaics were generated, which grouped about 47 sheets (paper) 1:1 scale, in the Adobe PhotoBridge software. In GIMP software, noise and drawing errors were eliminated, silhouettes were filled with color and the RGB information was converted in a binary model of one bit per pixel (black and white). In the software, the leave regions were recorded in black as shown in Figure 10 and 11. It is important to emphasize that in this step the dimensions of the mosaic are bounded, identifying the exact measurements of each side. This information is used in referencing and locating the resulting vector model. Following this, data is exported in files with referencing capabilities (such as TIF, TIFF), for their geometric correction in any geographic information system. In

this step, GRASS 6.4 software was used. If the file of exported data does not contain boundary capabilities, it is still possible to perform the procedure incorporating the manipulation of the TIC information of the resulting vector file. A description of this process can be found in (37). In the same software, the binary export file in TIF format is projected again under the Transverse Mercator coordinate system, with WGS84 datum, factor scale one and zero valued parameters. Thus, the sub meter accuracy necessary for adequate representation of the leaves in vector format is ensured. With the GRASS 6.4 command `r.to.vect`, and the enabled area option, the drawn objects vector model is obtained for further editing and creation of area and perimeter attributes. It is important to highlight the importance of the proper use of the tolerances for vector files, which must be less than 0.0003 m in order to avoid the modification of the model vertex.

The standard output of this process is shown in Figure 12. Furthermore, to ease the illustration of complex or divided leaf information; it must be carefully reconstructed for the preparation of the final matrices. In this way the fact that the leaf area truly corresponds to its record and not to a leaflet or part of the leaf is ensured. An additional benefit of this procedure is the ability to analyze, with any geographical information system, estimated records in the leaves, with the same methodologies used in landscape ecology. Metrics such as fractal dimension, perimeter area ratio, complexity, core analysis, and shape indices, among others, are equally applicable at this level. The results of this analysis will be presented in subsequent contributions.

With this procedure results, a matrix in which the two-dimensional leaf morphology is resumed is constructed. By multiplying element by element, the layer thickness records are incorporated in order to obtain the final volume matrix. This matrix is multiplied with the leaf count matrix, to obtain as an intermediate result, the foliar volume grouped in different

sizes provided by each individual. The subsequent steps were similar to those made for the other plant organs, with the difference that the leaf volume matrix was multiplied element by element with the corresponding hydrated and dry density's estimate to each calculated volume, later adding rows and estimating the total hydrated and dry biomass contribution by each individual.

The total surface contributed by the leaves was estimated with the multiplication of their count and the surface of each layer. The total area of each leaf results as the sum of the two layer sides with the product of the leaf perimeter and thickness. In this way, a more precise surface estimation that intervenes more actively in gas exchange is obtained, creating a breakthrough in the future understanding and calibration of atmospheric variables such as water vapor, gas exchange, breathing and transpiration, among others. The analysis of this information was excluded since its contribution is not part of the objectives of the present paper.

Finally the leaves of the species *Astrocaryum malybo*, *Attalea butyracea*, *Oenocarpus bataua*, *Sabal mauritiiformis*, *Socratea exorrhiza* and *Wettinia hirsuta*, were modelled following the same techniques used for stems and branches, led by field notes, photography and reconstruction of vector files to complete the matrix of areas and volumes (Figure 13).

### **Tree models classification based on their architecture.**

There are several ways to classify tree architecture such as: growth characteristics, main branches, split, apical branch growth, location of meristem growth, types of secondary branches and other characteristics such as leaf arrangement and leaf angles as distributed in the branches. One classification system of tree architecture, that stands out is that one proposed by (38) in which these characteristics are grouped into general architecture models, and highlights the main features of the structural and spatial configuration that are

acquired by different tropical species. According to (39) to perform this classification task, by trying to identify these features is not an easy task, and even more when it is known that many species alternate different growth characteristics, or lose in their maturity features the visible ones in juvenile phases. Furthermore, (39) makes a reclassification of procedures developed in (38) seeking to correct ambiguities in species and unite some architecture types, which are almost indistinguishable in adulthood. To adjust the characteristics of some types of branching in three-dimensional models, and secondly, to relate them with the possible causes of variability in biomass estimation, (30) classification was used, which incorporates an improved description of (38) architecture models and resolves the ambiguities presented in these.

In the classification of tree architecture, a matrix was generated in which information on the overall growth pattern, the architecture group, and the main features were stored. Species that generally showed a monopodial growth acquired a value of 1, i.e. meaning that a leading stem is identified, or a main growth axis (hipersilepsia) in comparison with the lateral apical meristems. Instead, sympodial growth was registered with a value of zero, when a growth pattern was quantified with evidence that a lateral one substituted the apical meristem or in case that several leader branches were identified. The branching patterns of the monopodial trunk were classified into the types as observed in the Supplementary note S3 (30).

### **Comparison between voxelisation methods and numerical integration**

The overall results of the volume estimation obtained with the methods of voxelisation and uncalibrated numerical integration, were adapted to perform a reliability analysis Kappa Cohen and quality ROC (40), in order to assess the most sensitive volumetric classification regarding the calibrated values (units in cubic centimeters). For the reliability analysis, a

typical confusion matrix was generated without modifying the records, and for the quality analysis, the proximity of the raw results between zero (0) and 800 cm<sup>3</sup> to the calibrated value was considered positive (labeled zero, true negatives), and as negative, (false positive marked with one), all records not found within these limits. As discussed in the methodology, in the voxelisation calculations and basically due to computational limitations, the use of different cubic units was employed, situation which, just as it happens with technologies based on pixel analysis (Raster), it is expected that the best results are found with datasets that present high density (resolution), which in this case correspond to models that generally present dimensions limited by 15 m long. Given these considerations, the test results show the percentage contributed by the methodologies in volume estimation without calibration, and within these results (volumes), which sectors are better represented by one or another methodology (with no calibration). It is worth mentioning that the records that contributed the most in the correction of inconsistencies caused by the election of different measurement units, mostly belong to the branch estimation (secondary branches) in cubic centimeters of the different modelled species.

The results of the volume obtained for each modelled species through the applied methods show, regarding precision, the highest reading in the concordance force was produced by the voxelisation methodology with Kappa = 0.6315 (Kappa = 0.4342 numerical integration), while for the ROC quality, the highest record was presented by the method of volume estimation by numerical integration with an area under the curve of 0.9560 with confidence interval, CI [0.9285 0.9834] (voxelisation area under the ROC curve = 0.91447 CI [0.8667 0.9623]) Supplementary note S4. As shown in Figure 14, it appears to be that the numerical integration method exceeds the quality of the estimations of the voxelisation

method because it has a lower rate of false positives and greater specificity for the evaluated volumes. However, due to the arguments shown throughout the study, and the exhibited knowledge of the benefits of the voxelisation method, these results should be reinterpreted. Since the ROC method is evaluating a wide range of volumes (between 82 cm<sup>3</sup> and 155,116,759 cm<sup>3</sup>), and since doubling the height implies a cubic volume increase and that due to technological limitations, the quality of the results obtained with the voxelisation method is focused at lower volumes (between 82 cm<sup>3</sup> and 2,403,575 cm<sup>3</sup>); it is concluded that the range of accuracy of this method relies on the lowest rates of true positives. This is why, the quality of the numerical integration method is exacerbated due to the fact that because of its vector features, it is limited by height and volume. Thus, the definition of a wider sector in the evaluated results is achieved. At this point, it is important to emphasize that the method of numerical integration in comparison to the voxelisation one, reached minimum differences, when the following features were met: the tree was represented by a homogeneous mesh model for all modelled organs (vector structure of vertex, normals and faces) and when the voxelisation was performed with cubic centimeter units. This also leads to the conclusion that homogeneous mesh models allow the adequate volume estimation with the numerical integration method, although once again limited by the available computing capacity.

### **Validation of the estimation methods**

The validation process consisted of volume comparisons of 10 individuals of *Aphelandra pulcherrima* with heights from 1.54 m to 2.9 m, using the techniques of cutting, weighing and green volume calculation by water displacement with a micro-graduated probe tube (Figure 15). The average volume by water displacement was 1,240 cm<sup>3</sup>, by numerical integration it was 1,217.76 cm<sup>3</sup> (1.798% difference), by voxelisation was 1,211 cm<sup>3</sup> with

one centimeter resolution (2.338% difference) and voxelisation with one millimeter resolution was 1,189.92 cm<sup>3</sup> (4.038% difference).

### **Method comparison with other studies and methodologies**

The assessment of vegetation structure and the variation of the biomass estimation by the traditional methodology, was explored in (14), which underlines the present work. Data was explored using descriptive statistical analysis and, frequency distributions, central tendency measures and biomass distribution were assessed by means of the basal area, density (number of elements) and the height of individuals belonging to 12 types of forest, among which the following associations are present: Jacarando copaiaie - Pouterietum multiflorae (super-humid), Protio aracouchini - Viroletum elongatae (very humid), Trichilio hirtae-Schizolobietum parahibi (humid) and the community of *Acalypha sp.* & *Guazuma ulmifolia* (semi-humid). On the other hand, results from different models were compared in order to choose the best allometric model to provide a better fit between DBH, height and specific weight of the wood. Chave *et al.* models (4) were chosen, since besides presenting a good apparent fit, they evaluate DBH intervals between 5 and 156 cm as well as the biomass estimation in tropical wet and dry forests.

In Colombia, Alvarez *et al.* (16) published some edited versions of the equations of Chave *et al.* (4) which show a similar trend, and increase the biomass estimates using the latter formulas.

In order to compare the results found in this study, using the methodology that integrates three-dimensional modelling, numerical integration, voxelisation and the data collected in the field from small samples (approximately 1 cubic inch per organ), with the biomass estimation as a result from the traditional allometric methodology, a comparison of covariance was performed, in which it is assumed that the biomass matrix found in this

study ( $\mathbf{X}$ ) corresponds to a simple random sample of size  $n_x$ , from a normal multivariate law  $X \sim N_m(\mu_x, \Sigma_x)$  and that the matrix  $\mathbf{Y}$  (biomass matrix found by the allometric equations) corresponds to another simple random sample independent from the previous one, of size  $n_y$ , from a multivariate law  $Y \sim N_m(\mu_y, \Sigma_y)$ . Equality of Covariance was evaluated by the contrast of hypothesis (41)  $H_0 : \Sigma_x = \Sigma_y = \Sigma$ . The contrast likelihood ratio was used in this case, which is found by the equation two.

$$\text{Equation 2. } \lambda_R = \frac{|S_x|^{\frac{n_x}{2}} |S_y|^{\frac{n_y}{2}}}{|S|^{\frac{n}{2}}}$$

Where  $S_x$  and  $S_y$  represent the sampled covariance matrices in each group,  $n = n_x + n_y$  and  $S$  are the common covariance matrix, found by weight (41). Under the null hypothesis it is given that  $-2 \log(\lambda_R) \sim \chi^2_q$ , where,  $q = \frac{(g-1)p(p+1)}{2}$  taking into account that

$$-2 \log(\lambda_R) = n * \log |S| - (n_x \log |S_x| + n_y \log |S_y|) \quad (39).$$

Thus, the null hypothesis is rejected if the value of this statistic belongs to the critical region  $[x_{1-\alpha}, +\infty)$ , where  $x_{1-\alpha}$  represents the percentile- $\alpha$  (1- $\alpha$ ) 100%. When the null hypothesis of equal covariance test is not rejected, we proceeded to perform a comparison of means by contrasting null hypothesis  $H_0 : \mu_x = \mu_y$ , using the statistic based on the  $\Lambda$  distribution of Wilks,  $\Lambda(p, n-g, g-1)$ . The statistical was found by the formula

$$\Lambda = \frac{|W|}{|B+W|} = \frac{|W|}{|T|}, \text{ where } W = n_x S_x + n_y S_y \text{ is the scattering matrix within groups and}$$

$B = n_x (\bar{X} - \bar{Z}), (\bar{X} - \bar{Z}) + n_y (\bar{Y} - \bar{Z}), (\bar{Y} - \bar{Z})$ , is the scattering matrix between groups.

$T = W + B$ , is considered the total scattering matrix, which contains the global mean vector

$$\bar{Z} = \frac{n_x \bar{X} + n_y \bar{Y}}{n} \quad (41).$$

### **Samples acquisition for carbon analysis.**

To determine the carbon content in the four vegetation communities analyzed, all woody individuals with GBH (Girth at Breast Height) greater or equal than 5 cm, were counted in sampling plots of 500 m<sup>2</sup>. In addition to the typical structural information (GBH, height and coverage) for each individual suggested in (42), samples were taken from each of the individual organs to the carbon analyzer. Each stem sample was obtained by extracting a small core of an inch in diameter with depths ranging from 1 to 5 cm (bark). Sizes were defined according to the thickness of the trunk, as well as causing the least harm to the individual. In small individuals, the sample never exceeded 1 inch in depth by one inch in diameter. The stem bark content of the latter was separated and added to the respective sample; usually obtained by scraping an area of up to 20 cm<sup>2</sup>. For the numerous organs, like leaves and branches, three samples per organ were taken in order to obtain replicas, and their number was determined based on the cost of the analysis. It is worth mentioning that, to capture some branches and leaves samples in portly individuals, it was necessary to establish transects of 100 m<sup>2</sup>, or tissue acquisitions in floristic routes in sites of similar physical conditions.

Thereafter, samples followed a dry and fresh weighing processes (samples dried at 80 ° C), and a volume calculation by displacement of water in a micro graduated probe test tube. A total of 2.232 samples of 0.02 g belonged to 186 individuals were processed and dried again at 105 ° C in an automatic analyzer LECO CHN-600 (14, 15, 43).

With the LECO analyzer, the full content of the carbon tissues was obtained by a combustion at 950 ° C (14, 15, 43). The sensitivity of 0.01 % generated by the instrument, is of great importance in the regional assessment of the elements content in the different vegetation communities, and by being sourced from a calibrated quantification method, it differs substantially from other methods such as LOI (Loss On Ignition), which not only requires bulk samples, but incorporates a major registry error by relying on the records of several weighing processes conducted by the researcher. For its proper usage, the LOI method requires the use of an analytical balance and collection of large number of replicas to generate the calibration curves by species. To obtain data for the LECO analyzer, only 0.02 g of sample is required and the monitoring of every 10 samples with standard low cost organic targets, such as ethylenediaminetetraacetic acid (EDTA), sucrose and leucine, with a known carbon content, in order, if necessary, to make small adjustments and keep up the process calibrated (14, 15, 43).

## **End notes**

### **Supplementary Information**

### **Acknowledgements**

Part of this work was funded by the Bicentennial project of the National University of Colombia, and received support from the Colombian Geological Service for elemental tissue samples analysis. We thank our student, Adela Vasquez Lozano MSc, for her active participation in various phases of the project.

### **Author contributions**

The study idea, research design, aboveground carbon sampling design, development methodology, data analysis and preparation of the figures of the main article and

supplementary information were provided by H.A.P. O.R.C. was responsible for the collection and preparation of structural data, for conducting the local phytosociological analysis that supported this study and for the provision of conditions for carrying out the research H.A.P. wrote the paper and interpreted the results, and both authors reviewed the manuscript.

### **Author information**

The authors declare no competing financial interests, details accompany the full-text HTML version of the paper at ([www.colombiaversidadbiotica.com](http://www.colombiaversidadbiotica.com)). There is no commercial filiation between the authors and the entities referred, thus no possible commercial use of the information presented in this document without the principal author consent is allowed. Commons Attribution-NonCommercial-ShareAlike 4.0 International (CC BY-NC-SA 4.0). Correspondence and requests for materials should be addressed to [harellano@unal.edu.co](mailto:harellano@unal.edu.co).

## References

1. Baccini, A. *et al.* Estimated carbon dioxide emissions from tropical deforestation improved by carbon-density maps. *Nature Clim. Change* **2**, 182-185; DOI:10.1038/nclimate1354 (2012).
2. Chave, J. *et al.* Improved allometric models to estimate the aboveground biomass of tropical trees. *Global Change Biol.* **20**, 3177–3190. DOI:10.1111/gcb.12629 (2014).
3. Feldpausch, T. R. *et al.* Tree height integrated into pantropical forest biomass estimates. *Biogeosciences* **9**, 3381-3403; DOI:10.5194/bg-9-3381-2012 (2012).
4. Chave, J. *et al.* Tree allometry and improved estimation of carbon stocks and balance in tropical forests. *Oecologia* **145**, 87-99; DOI:10.1007/s00442-005-0100-x (2005).
5. Overman, J. P. M., Witte, H. J. L., & Saldarriaga, J. G. Evaluation of regression models for above-ground biomass determination in Amazon rainforest. *J. Trop. Ecol.* **10**, 207–218; DOI:10.1017/S0266467400007859 (1994).
6. Sileshi, G. W. A critical review of forest biomass estimation models, common mistakes and corrective measures. *Forest Ecol Manag.* **329**, 237–254; DOI:10.1016/j.foreco.2014.06.026 (2014).
7. Asner, G.P. Tropical forest carbon assessment: integrating satellite and airborne mapping approaches. *Environ Res Lett.* **4**, 1-11; DOI:10.1088/1748-9326/4/3/034009 (2009).
8. Schulze, E. D., Wirth, C. & Heimann, M. Managing forests after Kyoto. *Science* **289**, 2058-2059; DOI:10.1126/science.289.5487.2058 (2000).
9. IPCC. *Guidelines for National Greenhouse Gas Inventories*. Prepared by the National Greenhouse Gas Inventories Programme, Eggleston, H. S. *et al.*, IGES, Japan (2006). Available at: <http://www.ipcc-nggip.iges.or.jp/public/2006gl/spanish/> (Accessed: 6th March

2011).

10. Avella-M., A & Rangel-Ch., J.O. Composición florística y aspectos estructurales de la vegetación boscosa del Sur del departamento de Córdoba. En: J.O. Rangel-Ch. (ed).

*Colombia Diversidad Biótica XII. La región Caribe de Colombia*. ICN, UNAL. Bogotá. 12, 447-537. (2012). Available at:

[http://www.colombiadiversidadbiotica.com/Sitio\\_web/Bienvenida.html](http://www.colombiadiversidadbiotica.com/Sitio_web/Bienvenida.html). (Accessed: 4th October 2011).

11. Rangel-Ch., J.O., Garay-P., H. & Avella-M., A. Bosques húmedos y secos circundantes a los complejos de humedales (ciénagas), en el departamento de Córdoba. En: J.O. Rangel-Ch. (ed). *Colombia Diversidad Biótica IX. Ciénagas de Córdoba: Biodiversidad ecológica y manejo ambiental*. ICN, UNAL. Bogotá. 9, 207-323. (2010). Available at:

[http://www.colombiadiversidadbiotica.com/Sitio\\_web/Bienvenida.html](http://www.colombiadiversidadbiotica.com/Sitio_web/Bienvenida.html). (Accessed: 4th May 2011).

12. Arellano-P, H. & Rangel-Ch., J.O. Preprint: CCA-Fuzzy-Land Cover and its implication in deforestation analysis: new method used for the classification of vegetation types and coverages. arXiv:1508.01916 [q-bio.QM],1-60 (2015).

13. Overman, J.P., Saldarriaga, J.G. & Duivenvoorden, J.F. Estimación de la biomasa aérea en el bosque del medio Caquetá, Colombia. *Colombia Amazónica* **4**, 135-147 (1990).

14. Vásquez, A. & Arellano, H. Estructura, biomasa aérea y carbono almacenado en los bosques del sur y noroccidente de Córdoba. en: Rangel-ch. J.O. (ed). *Colombia Diversidad Biótica XII. La región Caribe de Colombia*. 923-961. Instituto de Ciencias Naturales, Universidad Nacional de Colombia. Bogotá. arXiv:1208.0248v1 [q-bio.QM] (2012).

15. Vásquez-L., A. Cuantificación del carbono almacenado en los bosques del Sur y Noroccidente del departamento de Córdoba, Colombia. Tesis de Maestría en Biología.

Instituto de Ciencias Naturales, Universidad Nacional de Colombia. Bogotá. (2012).

16. Álvarez, E. et al. Tree above-ground biomass allometries for carbon stocks estimation in the natural forests of Colombia. *Forest Ecol Manag.* 267, 297-308; DOI:

10.1016/j.foreco.2011.12.013 (2012).

17. Simard, M., Pinto, N., Fisher, J., Baccini, A. Mapping forest canopy height globally with spaceborne lidar. *J. Geophys. Res.* **116**, G04021, 12 PP; DOI:10.1029/2011JG001708 (2011).

18. Mitchard, E. T. A. et al. Markedly divergent estimates of Amazon forest carbon density from ground plots and satellites. *Global Ecol. Biogeogr.* **23**, 935–946.

DOI:10.1111/geb.12168 (2014).

19 Rutishauser, E. et al. Generic allometric models including height best estimate forest biomass and carbon stocks in Indonesia. *Forest Ecol Manag.* **307**, 219–225;

DOI:10.1016/j.foreco.2013.07.013 (2013).

20. The Woods Hole Research Center. Pantropical National Level Carbon Stock Dataset.

Available at: [http://www.whrc.org/mapping/pantropical/carbon\\_dataset.html](http://www.whrc.org/mapping/pantropical/carbon_dataset.html). (Accessed: 5th December 2013).

21. Zarin, D.J. Carbon from Tropical Deforestation. *Science* **336**, 1518-1519;

DOI:10.1126/science.1223251 (2012).

22. Ketterings, Q., Coe, R., van Noordwijk, M., Ambagau, Y. & Palm, C. Reducing uncertainty in the use of allometric biomass equations for predicting above-ground tree biomass in mixed secondary forests. *Forest Ecol Manag* **146**, 199-209;

DOI:10.1016/S0378-1127(00)00460-6 (2001).

23. Mirtich, B. Fast and Accurate Computation of Polyhedral Mass Properties. *JGT* **1**, 1-15;

DOI:10.1080/10867651.1996.10487458 (1996).

24. Gosline, A. Ported to Matlab Mirtich. Volume Integration (1997). [code]. Available at: <http://www.cim.mcgill.ca/~andrewg/volumeIntegration.m>. (Accessed: 4th October 2011).
25. Patil, S. & Ravi, B. Voxel-based representation, display and thickness analysis of intricate shapes. Ninth international conference on computer aided design and computer graphics (CAD/CG 2005). 6 p. DOI:10.1109/CAD-CG.2005.86 (2005).
26. Aitkenhead, A. VOXELISE.m. The Christie NHS Foundation Trust. (2011). [code]. Available at: [http://www.mathworks.com/matlabcentral/fileexchange/27390-mesh-voxelisation/content/Mesh\\_voxelisation/VOXELISE.m](http://www.mathworks.com/matlabcentral/fileexchange/27390-mesh-voxelisation/content/Mesh_voxelisation/VOXELISE.m) (Accessed: 4th October 2011).
27. Elias, M. & Potvin, C. Assessing intra and inter specific variation in trunk carbon concentration for 32 neotropical tree species. *Can J Forest Res.* **33**, 1039-1045; DOI:10.1139/X03-018 (2003).
28. Lamtom, S.H. & Savidge R.A. A reassessment of carbon content in wood: variation within and between 41 North American species. *Biomass Bioenerg.* **25**, 381–388; DOI:10.1016/S0961-9534(03)00033-3 (2003).
29. Zhang, J. *et al.* Carbon concentration variability of 10 Chinese temperate tree species. *Forest Ecol Manag.* **258**, 722–727; DOI:10.1016/j.foreco.2009.05.009 (2009).
30. Keller, R. *Identification of tropical woody plants in the absence of flowers and fruits. A field guide. 2nd edn.* (ed. Keller, R.) 340 pp. (Birkhauser, 2004).
31. Gentry, A.H. Changes in plant community diversity and floristic composition on environmental and geographic gradients. *Ann Mo Bot Gard.* **75**: 1-34. (1988). Available at: <http://www.jstor.org/stable/2399464>. (Accessed: 9th May 2012).
32. Boyle, B.L. *Changes on Altitudinal and Latitudinal Gradients in Neotropical Montane Forests.* (ed. Boyle, B.L) 275 pp. (Washington University, 1996).
33. Arellano-P., H. Servicios ambientales de la biodiversidad-Almacenamiento de carbono

- y deforestación evitada en áreas del Caribe colombiano. Tesis Doctorado en Biología. Instituto de Ciencias Naturales, Universidad Nacional de Colombia. Bogotá. (2012).
34. Appel, A. Some techniques for shading machine renderings of solids. Proceedings of the April 30--May 2, 1968, spring joint computer conference. 37-45; DOI:10.1145/1468075.1468082 (1968).
35. Whitted, T. An improved illumination model for shaded display. Communications of the ACM 23, 343-349; DOI:10.1145/1198555.1198743 (1980).
36. Berdugo-L., M.L. Patrones biotipológicos a nivel foliar de la vegetación y su respuesta a las series hídricas en áreas de la región Caribe de Colombia. Tesis de grado. Facultad de ciencias. Universidad Nacional de Colombia. (2011).
37. Arellano-P, H. & Rangel, J. O. Fragmentación y estado de conservación en algunos páramos de Colombia. En J. O. Rangel-Ch. (ed). Colombia Diversidad Biótica X. El páramo colombiano, cambios globales y amenazas del cambio climático. Instituto de Ciencias Naturales, Universidad Nacional de Colombia. Bogotá. (2010). Available at: [http://www.colombiadiversidadbiotica.com/Sitio\\_web/Bienvenida.html](http://www.colombiadiversidadbiotica.com/Sitio_web/Bienvenida.html). (Accessed: 25th November 2009).
38. Halle, F. & Oldeman, A. A. Essai sur l'Architecture et la Dynamique de Croissance des Arbres Tropicaux. (eds. Halle, F. & Oldeman, A. A) Masson et Cie, Paris (Masson, 1970).
39. Leigh, E. G. J. Tropical Forest Ecology: A View from Barro Colorado Island. (ed. Leigh, E. G. J.) 245 pp. (Oxford Univ. Press., 1999).
40. Cardillo, G. ROC curve: compute a Receiver Operating Characteristics curve. (2007). Available at: <http://www.mathworks.com/matlabcentral/fileexchange/19950>. (Accessed: 4th April 2012).
41. Peña, D. Análisis de datos multivariantes. 1st edn, (ed. Peña, D.) 515 pp. (McGraw-

Hill, 2002).

42. Rangel-Ch., J.O. & Velásquez, A. Métodos de estudio de la vegetación. En: J.O. Rangel-Ch., P. Lowy & M. Aguilar (eds). Colombia diversidad biótica II. Tipos de vegetación en Colombia. 59-87. Instituto de Ciencias Naturales, Universidad Nacional de Colombia. Bogotá. (1997). Available at:

[http://www.colombiadiversidadbiotica.com/Sitio\\_web/Bienvenida.html](http://www.colombiadiversidadbiotica.com/Sitio_web/Bienvenida.html) (Accessed: 25th May 2009).

43. Sheldrick, B.H. Test of the leco CHN-600 determinator for soil carbon and nitrogen analysis. Canadian Journal of Soil Science. 66, 543-545; DOI:10.4141/cjss86-055 (1984).

**Table 1 | Summary of volume and biomass values per individual in the plots.**

ASSOCIATION	SYMBOL MAPPING (13b)	SPECIES	DB H (cm)	HEIGHT (m)	TOTAL VOLUME LEAVES (cm <sup>3</sup> )	TOTAL AERIAL BIOMASS (Kg)	TOTAL AERIAL BIOMASS EQUATIONS OVERMAN et al. (1990) (Kg)	TOTAL AERIAL BIOMASS EQUATIONS CHAVE et al. (2005) (kg)	ASSOCIATION	SYMBOL MAPPING (13b)	SPECIES	DB H (cm)	HEIGHT (m)	TOTAL VOLUME LEAVES (cm <sup>3</sup> )	TOTAL AERIAL BIOMASS (Kg)	TOTAL AERIAL BIOMASS EQUATIONS OVERMAN et al. (1990) (Kg)	TOTAL AERIAL BIOMASS EQUATIONS CHAVE et al. (2005) (kg)				
Jacaranda copaie-Pouterietum multiflorae	BHf2/Jco-Pmu	<i>Amphirrhox longifolia</i>	7.92	6.04	685.05	4.59	13.83	11.16	Protio aracouchini-Viroletum elongatae	BHhmf1/P-ar-Vel	<i>Protium aracouchini</i>	39.75	19.76	119038.86	1332.18	825.79	880.14				
		<i>Brosimum utile</i>	9.20	6.24	5597.63	4.67	20.24	17.19			<i>Pseudolmedia laevigata</i>	24.38	12.16	41774.76	441.08	219.13	226.10				
		<i>Crepidospermum rhoifolium</i>	5.49	7.84	2781.03	8.08	6.57	4.69			<i>Pterocarpus rohrii</i>	9.14	7.48	296640.81	35.51	16.81	13.93				
		<i>Dendrobangia boliviana</i>	29.87	21.06	357970.05	1245.04	527.42	559.05			<i>Qualea dinizii</i>	37.19	18.43	21082.39	1704.02	666.05	708.50				
		<i>Dendrobangia boliviana</i>	40.23	19.26	192102.28	2364.19	870.11	927.64			<i>Schefflera morototoni</i>	26.21	22.07	18.98	426.68	367.16	385.90				
		<i>Dialium guianense</i>	69.49	30.53	11151.79	25823.46	6240.60	6375.30			<i>Schizolobium parahyba</i>	32.92	19.16	74991.47	530.83	613.24	651.62				
		<i>Dipteryx oleifera</i>	81.69	30.29	95601.20	26112.26	7804.09	7882.48			<i>Simaba cedron</i>	16.46	10.27	5746.67	63.97	58.27	55.28				
		<i>Dipteryx oleifera</i>	163.92	36.42	130032.75	52314.84	42987.46	38161.36			<i>Sloanea brevispina</i>	26.82	16.18	56436.79	871.97	387.34	407.71				
		<i>Duguetia flagellaris</i>	12.44	15.54	1281.86	78.94	106.07	105.23			<i>Sorocea trophoides</i>	13.41	12.44	5065.13	31.64	72.42	69.93				
		<i>Eschweilera pittieri</i>	29.87	19.94	26882.91	1061.47	678.76	722.18			<i>Swarzta simplex</i>	12.80	9.06	4424.83	74.82	69.17	66.54				
		<i>Guarea gomma</i>	32.92	18.98	153538.76	454.17	466.06	492.79			<i>Tetragastris panamensis</i>	18.90	12.93	76500.16	183.20	151.91	153.98				
		<i>Guarea gomma</i>	43.89	17.03	722495.27	3043.05	738.24	786.15			<i>Theobroma glaucum</i>	3.66	2.84	19776.82	1.39	2.15	1.20				
		<i>Guarea sp 2</i>	3.47	4.35	10777.23	1.18	2.71	1.60			<i>Virola elongata</i>	4.88	4.19	2080.79	4.88	4.32	12.79				
		<i>Helianthostylis sprucei</i>	12.11	6.89	1040.06	55.35	34.87	31.51			<i>Virola elongata</i>	7.92	7.14	911.72	0.53	15.60	2.84				
		<i>Helicostylis tomentosa</i>	3.66	5.41	10805.71	4.59	3.69	15.87			<i>Virola elongata</i>	14.63	13.37	2359.45	115.74	83.62	81.61				
		<i>Helicostylis tomentosa</i>	9.14	5.86	29665.75	11.38	18.87	2.35			<i>Virola reidii</i>	5.49	9.17	8592.20	11.06	8.10	6.00				
		<i>Inga pilosula</i>	14.02	15.12	8992.04	143.14	72.55	70.05			<i>Virola reidii</i>	111.56	29.09	377991.33	10297.80	6997.34	7108.09				
		<i>Iryanthera hostmannii</i>	6.10	3.05	464.49	1.01	5.48	3.78			<i>Virola sebifera</i>	84.12	26.98	40686.00	8427.72	5032.68	5191.34				
		<i>Iryanthera hostmannii</i>	13.41	25.56	70792.74	1067.84	151.23	153.25			<i>Ampelocera macrocarpa</i>	9.14	9.16	2239.63	9.33	32.59	29.25				
		<i>Iryanthera hostmannii</i>	27.98	18.17	57268.97	1276.78	384.19	404.31			<i>Ampelocera macrocarpa</i>	29.87	19.79	14811.21	1113.50	634.10	674.10				
		<i>Jacaranda copaia</i>	37.19	25.60	2253.29	519.43	771.59	821.98			<i>Anacardium excelsum</i>	38.40	18.95	15060.63	739.64	612.09	650.38				
		<i>Lindackeria laurina</i>	27.43	20.79	26941.27	1413.18	421.62	444.76			<i>Anacardium excelsum</i>	61.20	11.36	844.87	150.64	928.43	990.06				
		<i>Micrapholis guyanensis</i>	39.01	21.16	25546.06	1145.76	1014.30	1081.81			<i>Annona spraguei</i>	34.75	19.54	150966.20	810.69	620.26	659.18				
		<i>Nectandra membranacea</i>	1.83	2.01	1091.46	54.38	0.50	0.17			<i>Aspidosperma curranii</i>	35.97	18.00	53409.16	1370.10	706.63	752.16				
		<i>Pentaclethra macroloba</i>	48.16	23.83	18330.91	5153.94	1875.04	1990.46			<i>Astronium graveolens</i>	22.56	13.29	37229.57	907.67	207.24	213.31				
		<i>Pouteria multiflora</i>	70.10	27.96	41809.83	7467.86	2743.95	2889.67			<i>Bombacopsis quinata</i>	28.04	14.78	90556.71	666.42	221.01	228.12				
		<i>Protium aracouchini</i>	11.03	17.42	483127.56	213.15	65.71	62.96			<i>Bursera simaruba</i>	39.62	21.19	471492.64	281.76	579.94	615.72				
		<i>Protium aracouchini</i>	34.75	20.90	109084.27	1658.91	703.81	749.14			<i>Bursera simaruba</i>	90.22	25.94	423216.08	4017.15	3745.98	3907.99				
		<i>Schefflera morototoni</i>	15.85	23.22	20.87	179.00	146.74	148.45			<i>Caesalpinia glabrata</i>	42.67	16.13	3022.12	1488.85	1157.50	1234.36				
		<i>Sorocea trophoides</i>	23.16	23.46	65211.60	731.90	374.13	393.43			<i>Castilla elastica</i>	33.53	20.23	133429.23	775.69	402.47	424.06				
		<i>Sterculia apetala</i>	16.46	12.09	237988.14	83.33	58.46	55.47			<i>Ceiba pentandra</i>	39.62	17.38	53443.27	135.64	394.10	415.01				
		<i>Swarzta robinifolia</i>	16.46	15.04	5258.29	603.04	178.61	182.56			<i>Ceiba pentandra</i>	197.51	40.44	195525.38	54351.06	25807.52	23995.74				
		<i>Theobroma glaucum</i>	18.29	10.98	21564.46	33.89	118.91	118.83			<i>Chrysophyllum lucenifolium</i>	9.75	10.08	45286.54	19.65	37.59	34.23				
		<i>Theobroma glaucum</i>	20.73	21.09	682692.48	299.09	281.23	293.05			<i>Chrysophyllum lucenifolium</i>	34.75	19.61	37632.68	908.81	793.45	845.44				
		<i>Trichilia sp 1</i>	2.99	3.00	171.61	0.11	1.59	0.82			<i>Cratava tapia</i>	17.07	14.08	33614.86	35.59	112.86	112.42				
		<i>Virola elongata</i>	21.34	14.03	2678.83	261.18	154.42	156.66			<i>Gyrocarpus americanus</i>	9.14	5.15	23737.54	12.62	6.25	4.42				
		<i>Virola elongata</i>	121.92	13.80	454611.24	607.98	5702.06	5849.72			<i>Hura crepitans</i>	176.78	47.92	238866.63	35121.83	36014.38	32512.16				
		Protio aracouchini-Viroletum elongatae	BHhmf1/P-ar-Vel	<i>Amphirrhox longifolia</i>	10.97	7.45	723.84	42.86			29.67	26.35	Trichilio hirtae-Schizolobium parahibi	BHf1/Thi-Spa	<i>Machaerium goudotii</i>	70.10	17.44	697.76	4182.66	3035.85	3188.23
				<i>Amphirrhox longifolia</i>	14.02	11.95	3454.47	235.00			71.60	69.07			<i>Marila laxiflora</i>	30.48	24.14	67911.25	612.44	447.21	472.42
				<i>Brosimum guianense</i>	38.40	24.45	25293.61	3192.35			2916.83	1323.35			<i>Pentaplaris dorsetiae</i>	10.36	10.38	12140.02	22.40	34.57	117.07
				<i>Brosimum guianense</i>	58.52	24.40	44034.98	5394.16			1241.30	3066.69			<i>Pentaplaris dorsetiae</i>	17.68	13.38	8707.46	8.40	117.25	31.21
				<i>Brosimum utile</i>	13.41	10.44	7889.47	22.22			63.91	61.09			<i>Pentaplaris dorsetiae</i>	90.22	28.04	404690.93	5726.41	6254.27	6388.59
				<i>Carapa guianensis</i>	7.92	14.01	169347.98	125.57			21.85	18.73			<i>Pouteria subrotata</i>	9.75	9.80	47343.19	38.12	36.08	32.72
				<i>Curatiana pyriformis</i>	57.30	30.06	3107.33	7700.54			2585.82	2727.23			<i>Pouteria subrotata</i>	21.95	11.53	61628.61	251.05	190.20	194.99
				<i>Curatiana pyriformis</i>	68.88	19.85	3632.20	2250.09			2464.89	2602.65			<i>Pseudobombax septenatum</i>	120.70	29.79	234312.72	16874.63	7513.78	7604.60
<i>Caryocar amygdaliferum</i>	23.77			6.39	39998.21	5.45	19832.29	106.60	<i>Rhus striata</i>	15.24	7.41	39148.21			136.58	54.14	51.03				
<i>Caryocar amygdaliferum</i>	123.75			41.71	423433.20	30362.98	107.36	18838.25	<i>Schizolobium parahyba</i>	41.45	19.63	79315.97			842.11	807.01	860.00				
<i>Castilla elastica</i>	8.53			7.97	33418.48	7.02	13.48	10.83	<i>Schizolobium parahyba</i>	60.35	27.63	62128.17			3573.41	2429.61	2566.26				
<i>Cavanillesia platanifolia</i>	79.86			37.03	329884.40	15519.07	5208.23	5364.57	<i>Sciadodendron excelsum</i>	45.72	15.70	360.59			831.51	642.73	683.39				
<i>Cecropia sp 2</i>	5.49			7.90	172.26	1.66	8.05	5.96	<i>Trichilia hirta</i>	9.75	6.52	10888.47			26.08	25.34	22.11				
<i>Compsoneura matisi</i>	14.02			7.06	4504.31	8.49	28.98	25.67	<i>Trichilia hirta</i>	54.25	26.88	14528.02			4379.04	2284.67	2416.44				
<i>Compsoneura</i>	15.21			12.34	4522.96	45.92	56.08	53.02	<i>Zanthoxylum</i>	9.75	8.19	6700.70			16.97	28.65	25.35				



**Table 2 | Comparison of the results of biomass estimation for the X matrix (DBH, height, biomass of the stem and the main branches, secondary branches or twigs, leaf biomass and total biomass three-dimensional modelling) and Y matrix (the same structural variables as X and the biomass of the organs estimated with allometric equations) (13).**

Forests established from super-humid to humid climates					
DBH intervals	Size nx and ny	H <sub>0</sub>	- 2log ( $\lambda$ R)	[x1- $\alpha$ , + $\infty$ )	p
0 and 20 cm	81		2511.54		
20 and 40 cm	44		1861.10		
40 and 60 cm	15	rejected	646.92	[24.99, + $\infty$ )	0.00
60 and 100	14		603.82		
Higher than 100 cm	8		335.42		
Forests established on semi humid climates					
0 and 20 cm	24		705.12		
20 and 40 cm	14		470.75		
40 and 60 cm	7	rejected	238.89	[24, 99, + $\infty$ )	0.00
Higher than 60 cm	8		413.65		

**Table 3 | Distribution of carbon stocks as storage intervals per hectare and general vegetation formation in pantropical regions.**

<b>Class</b>	<b>Carbon stocks interval (Mg C ha<sup>-1</sup>)</b>	<b>Type of vegetation formation</b>	<b>Carbon stocks (Pg)</b>	<b>Flat surface (ha<sup>-1</sup>)</b>	<b>Relation ship of carbon stocks and flat surface (ha<sup>-1</sup>)</b>	<b>Percentage</b>
5	478-605	<b>Forests with multiple layers in high conservation</b>	285.03	531,449,420.52	531.05	39.37
4	336-478		281.76	668,896,502.68	417.09	38.91
2	58-183	<b>Very disturbed forest and scrub forest formations and tall scrub</b>	105.54	419,412,183.77	249.16	14.57
3	183-336	<b>Secondary forests, moderately intervened forest and woodland formations interspersed with sheets</b>	40.66	350,688,503.17	114.80	5.61
1	1-58	<b>Sites dominated by savannah vegetation, forest fragments, or completely degraded forests, low shrubs.</b>	10.96	828,606,996.75	13.10	1.51
<b>Total</b>			<b>723.97</b>	<b>2,799,053,606.91</b>		

Mg: Megagrams; C: Carbon; ha<sup>-1</sup>: Hectare; Pg: Petagrams.

**Table 4 | Countries with high carbon stocks estimated using the methodology proposed in this work.**

Countries with high carbon stocks				Countries with high carbon stocks per unit area			
Country	Country area (km <sup>2</sup> )	Carbon stock (Pg)	Carbon per km <sup>2</sup>	Country	Country area (km <sup>2</sup> )	Carbon stock (Pg)	Carbon per km <sup>2</sup>
<b>Brazil</b>	8,507,128	194.24	22,833.45	<b>Equatorial Guinea</b>	27,085.30	1.16	43,107.19
<b>Zaire</b>	2,337,027	71.95	30,787.99	<b>Brunei</b>	5769.53	0.24	42,034.99
<b>Indonesia</b>	1,910,842	64.41	33,710.66	<b>Papua New Guinea</b>	466,161.18	19.45	41,741.36
<b>Colombia</b>	1,141,962	37.34	32,701.25	<b>French Guiana</b>	83,811.13	3.46	41,370.25
<b>Peru</b>	1,296,912	36.12	27,854.89	<b>Guyana</b>	211,241.29	8.60	40,741.44
<b>Bolivia</b>	1,090,353	28.82	26,439.54	<b>Suriname</b>	145,497.5	5.91	40,656.40
<b>Venezuela</b>	916,561	23.63	25,782.34	<b>Gabon</b>	261,688.70	10.53	40,249.97
<b>Papua New Guinea</b>	466,161	19.45	41,741.36	<b>Laos</b>	230,566.09	9.23	40,050.80
<b>México</b>	1962939	15.29	7792.11	<b>Liberia</b>	96296.03	3.63	37735.46
<b>Myanmar (Burma)</b>	669,820.87	12.96	19,354.38	<b>Malaysia</b>	330,269.59	12.22	37,009.20

Km<sup>2</sup>: Square kilometres; Pg: Petagrams.

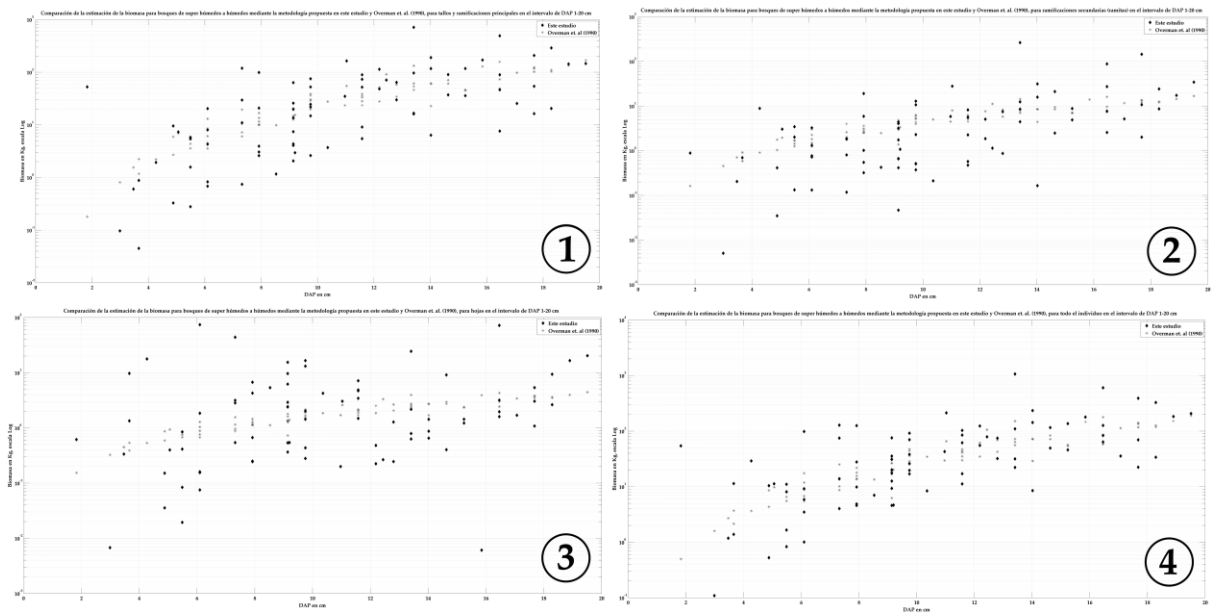


**Figure 1.** Comparison of the estimated biomass for forests established from super-humid to humid climates studied through the three-dimensional modelling methodology of the individuals (dark rhomboid), and the traditional allometric methodology published by Overman *et al.* (1990) (grey dots) for the different studied organs and each of the individuals in the DBH range from one (1) to 20 cm. For the preparation of the figure the software MATLAB 2011b was used.

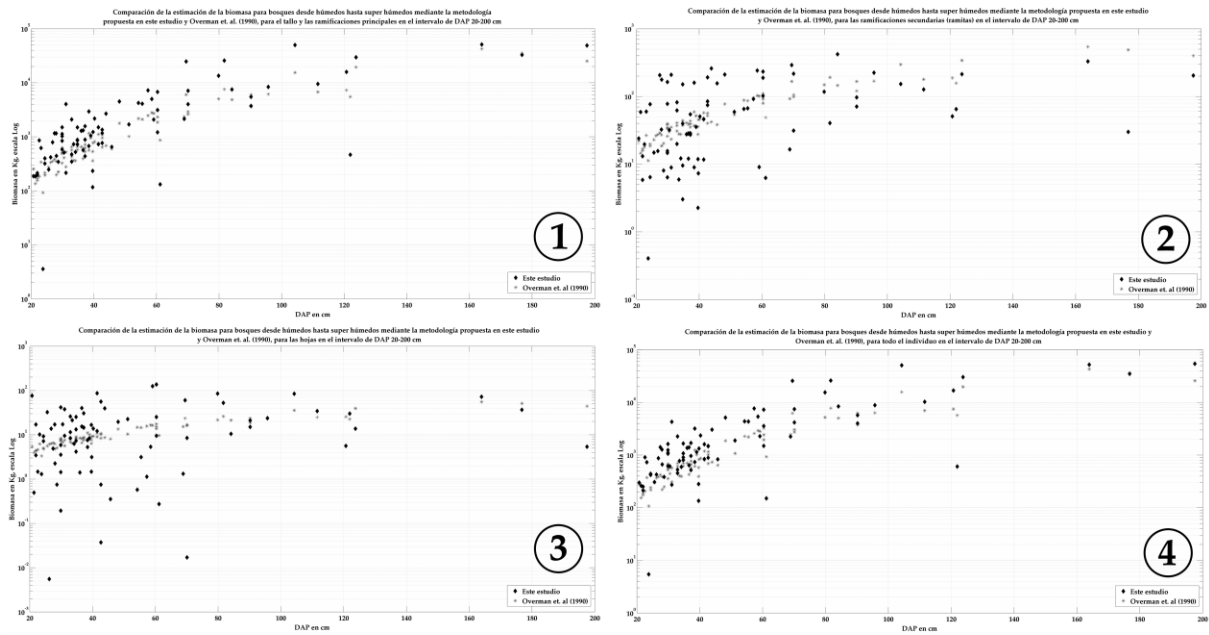


**Figure 2.** Comparison of the estimated biomass for forests established from super-humid to humid climates studied through the three-dimensional modelling methodology of individuals (dark rhomboid), and the traditional allometric methodology published by Overman *et al.* (1990) (grey dots) for different studied organs in the DBH range of 20 to 200 cm. The software MATLAB 2011b was used for the preparation of the figure.

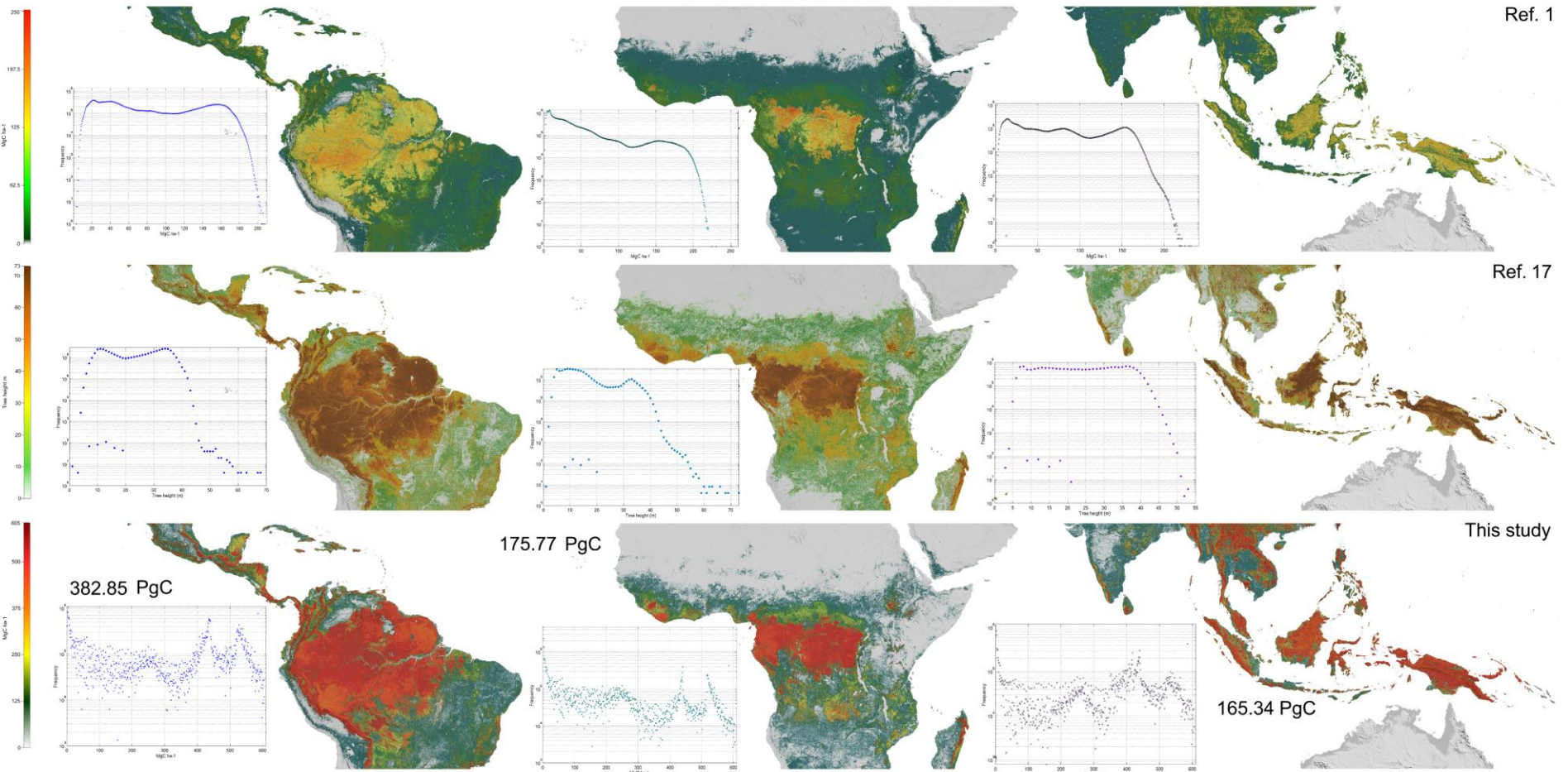


**Figure 3.** Calibration of pantropical carbon map estimated by implementing our methodology. The values above are in MgC per hectare per continent as in Ref. 1. The map data is produced by Baccini *et al.* (2012). In the middle, the distribution of tree height by continent is provided from Ref. 17. The map data is produced by Simard *et al.* (2011). The results

of the calibration of pantropical carbon map based on our methodology are below. Note the dispersal of the data attributed to the incorporation of different architectures in estimating carbon per hectare. The lower map is the result of modelling using neural network back-propagation for results obtained in this study and information from Ref. 1 (top) and Ref. 17 (middle). MATLAB 2011b was used by Arellano to process and present the distribution of frequencies in  $\text{MgC ha}^{-1}$  (logarithmic scale). The results were rendered by

Arellano in GRASS 6.4, and the composition was made with GIMP 2.6.

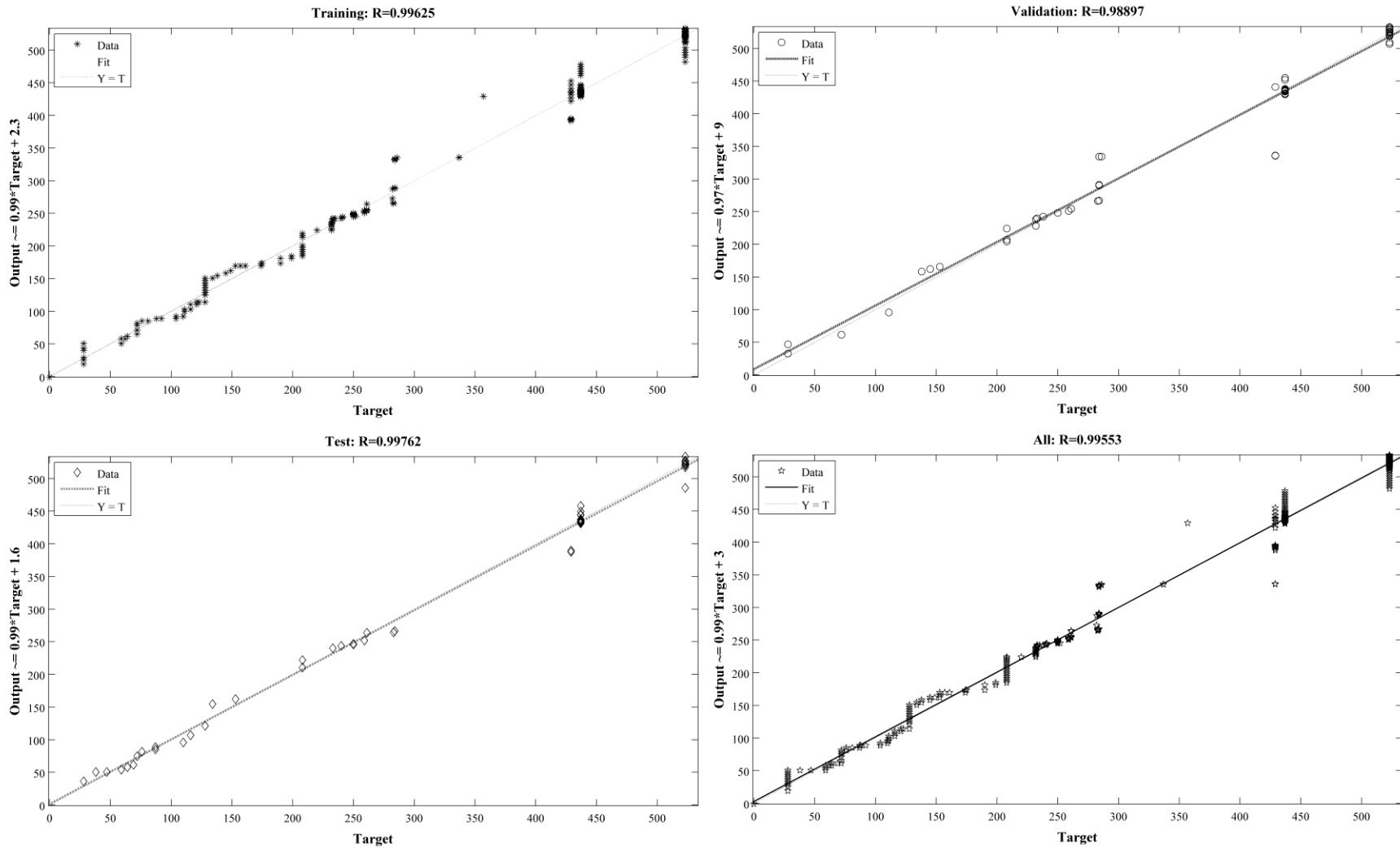


**Figure 4.** Data adjustment results from an artificial neural network. The data was transformed by a logarithmic sigmoidal function with linear output. In addition to the adjustments made to the data used in training, the system randomly chose a group of records to test the validation. Another similar test was performed using random values located in the range of DBH evaluated. The end result is the correlation coefficient among all tests. This approach allowed the selection of the neural models that gave the best explanation of the evaluated records. MATLAB 2011b software was used to prepare the figure.

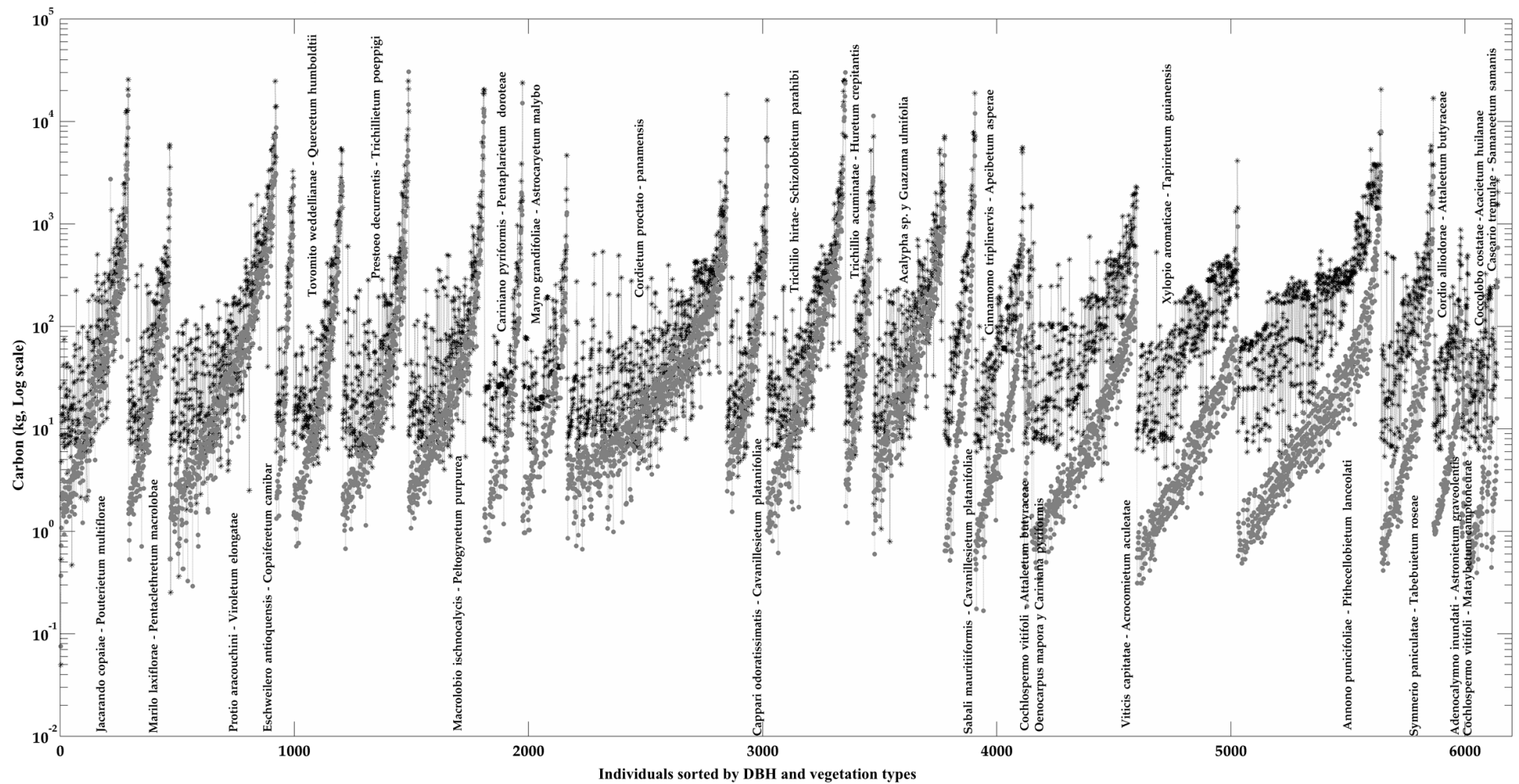


**Figure 5.** Results in kilograms (logarithmic scale) of the estimated carbon content for more than 6,000 individuals of different species belonging to 27 vegetation types in the studied area. Results obtained using the methodology based on three-dimensional modelling (dark asterisk) and calibration using artificial neural networks are contrasted, and the values were found by applying the equations of (4) (grey dots). MATLAB 2011b software was used to prepare the figure.

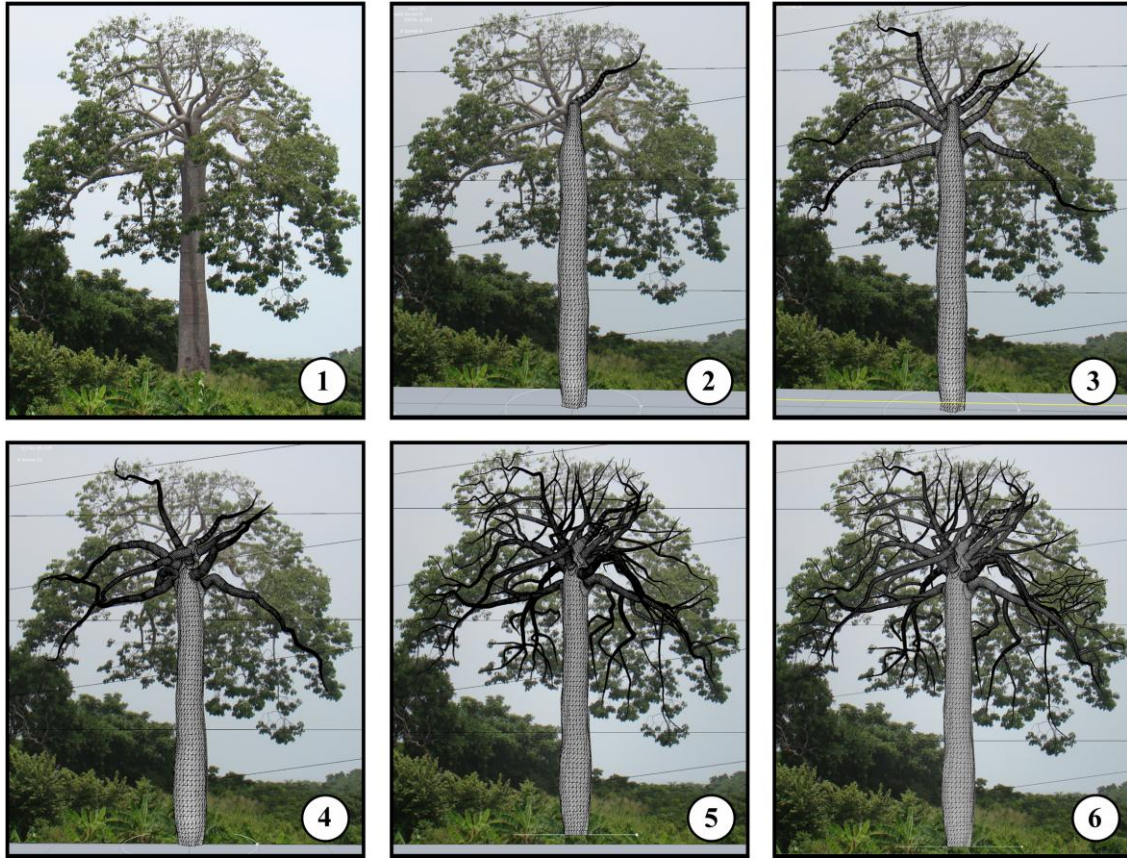


**Figure 6.** Building process of bounded three-dimensional model of the fourth level branching system in an individual of *Cavallinesia platanifolia* (Güipo, Volado, Macondo). The fifth and sixth levels are modelled separately to expedite the calculation process. In one (1) the individual to be modelled is observed, from two (2) to (3) the first surfaces without boundaries are observed (perspective view), and from four (4) to six (6), the stem and branch surfaces with size and position corrections (bounded model, XZ side view). Besides the traditional coverage measures, it is advised to use a lateral photo (YZ) or a side angle shot, to correct the nodes position of the Bezier curves and obtain optimal results. For the preparation of the figure SpeedTree 6.1.1 was used.

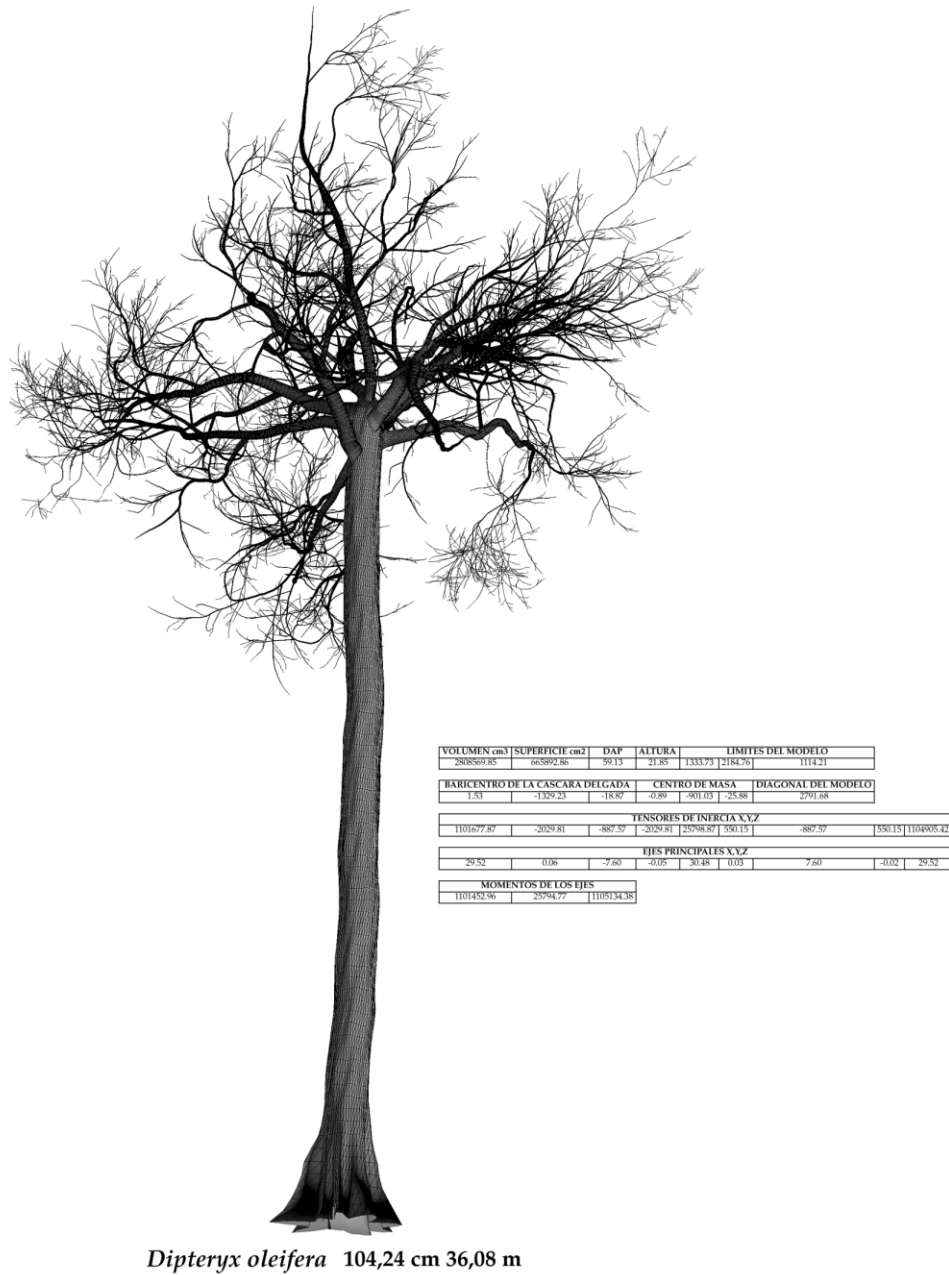


**Figure 7.** Mesh model of an individual of *Bursera graveolens* with 51.82 cm DBH and 9.32 meters high. The table shows the results of parameter estimation according to the method of numerical integration by Mirtich (1996). Code implementation and preparation of the figure MATLAB 2011b was used.

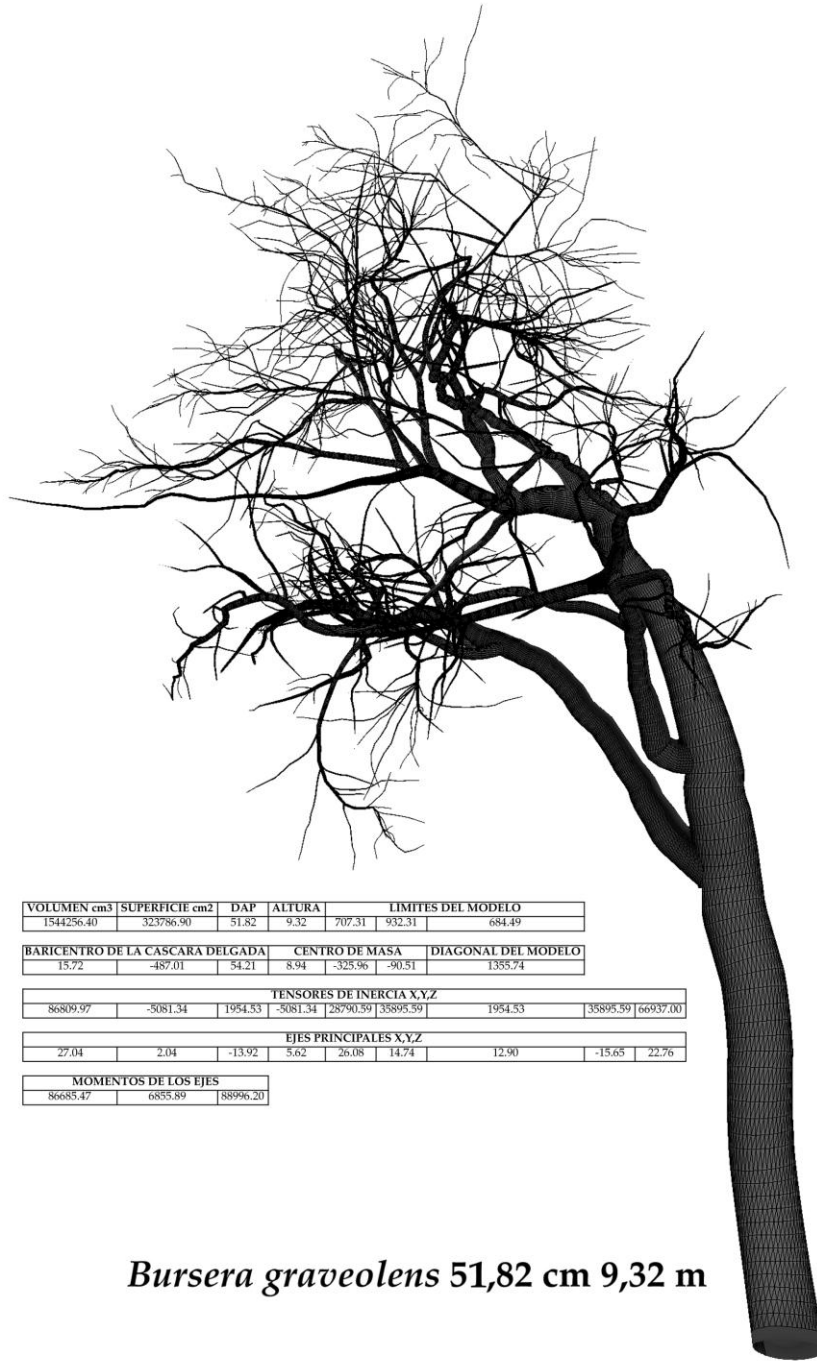


**Figure 8.** Mesh model of an individual of *Bursera graveolens* 51.82 cm DBH and 9.32 meters high. The table shows the results of parameter estimation according to the method of numerical integration by Mirtich (1996). In general, large trees with branches below two thirds of its height indicate anthropogenic disturbance conditions, due to the removal by man of competitiveness with others located in lower strata. MATLAB 2011b was used for the code implementation and preparation of the figure.

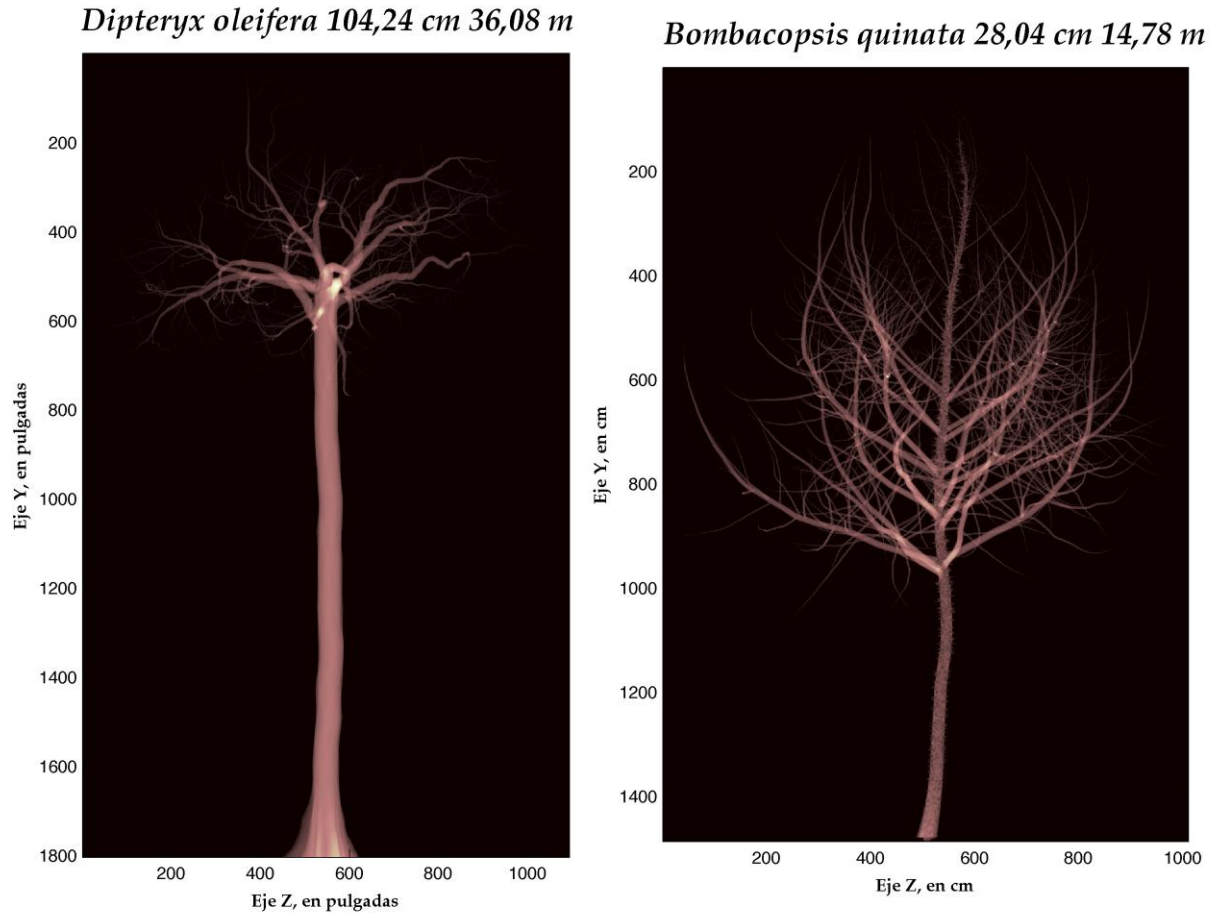


**Figure 9.** Voxel model of an individual of *Dipteryx oleifera* with 104.24 cm DBH and 36.08 meters high, and *Bombacopsis quinata* of 28.04 cm DBH and 14.78 m high, generated by modifying Aitkenhead's (2011) code. MATLAB 2011b was used for the code implementation and preparation of the figure.

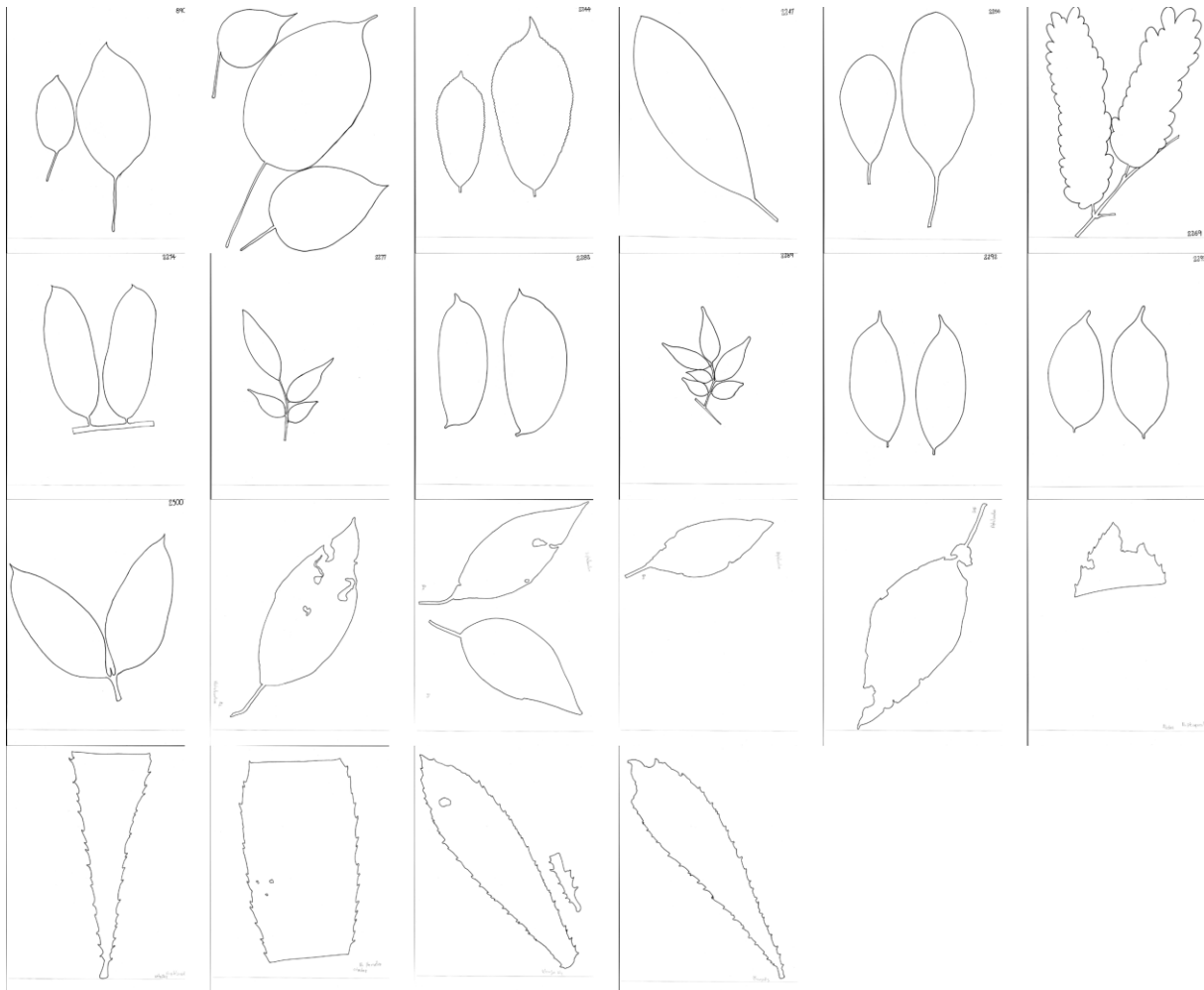


**Figure 10.** Ink silhouette captures of individuals belonging to different species. The most important layer features are seen including the herbivory. Information of complex or divided leaves divided was carefully reconstructed for the elaboration of final matrices to facilitate their illustration. The results were rendered with GIMP 2.6.



**Figure 11.** Color filling result of positive leaf areas and some layer reconstruction. This is the aspect that information acquires in raster format (.TIF) of one bit per pixel. The results were rendered with GIMP 2.6

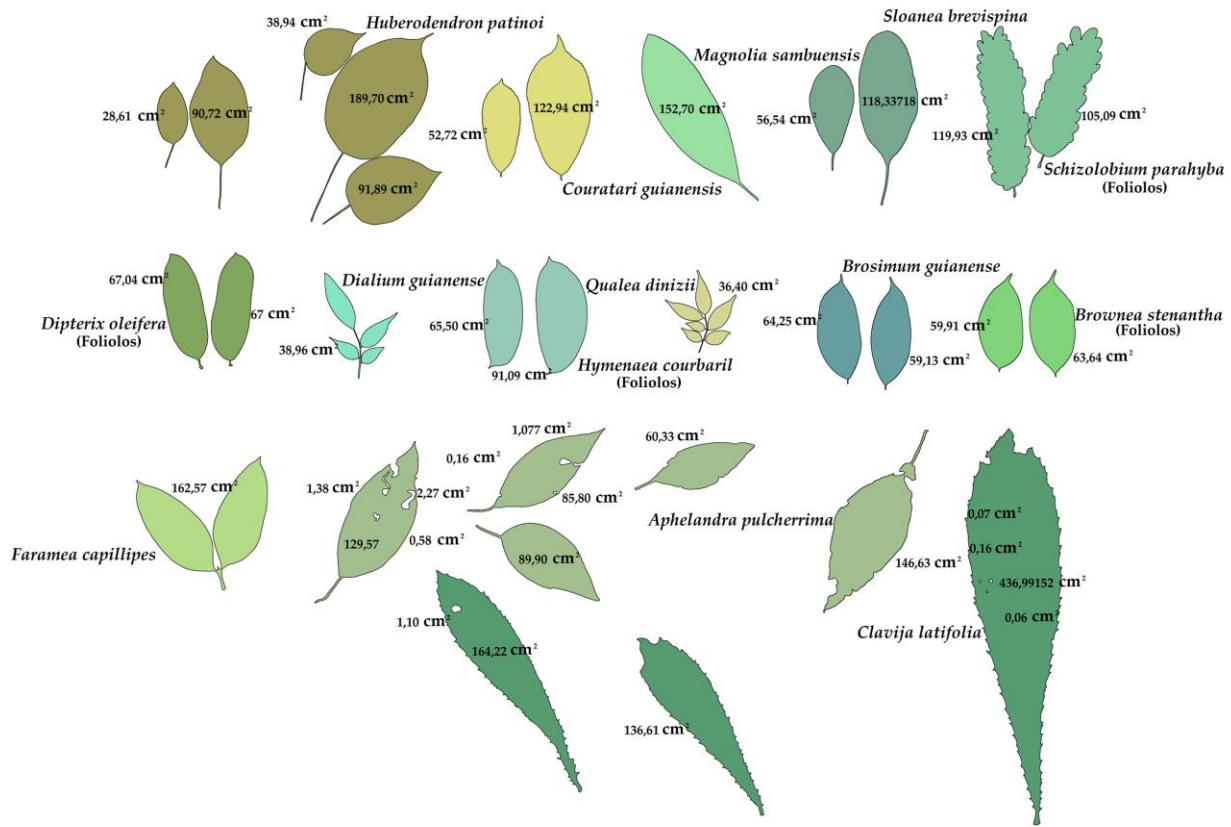


**Figure 12.** Results of the vectorization process of the leaf blades and some support structures. The attribute table shows which object belongs to a higher order structure (composite leaf) and which structure belongs to a layer segment. The figure shows the results of the area of one of the leaf’s face and the eaten surface by the action of herbivory. Results were performed using GRASS 6.4.

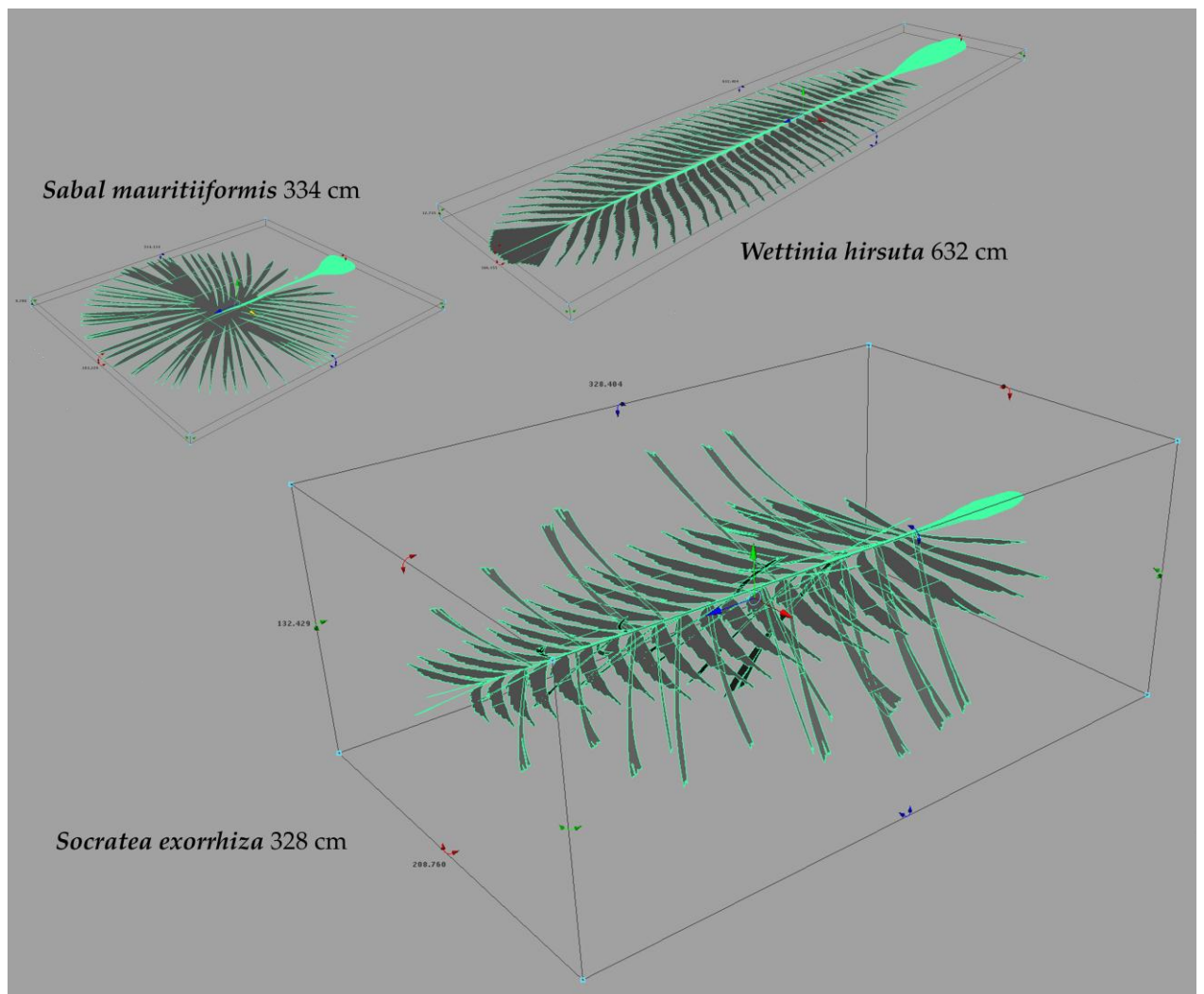
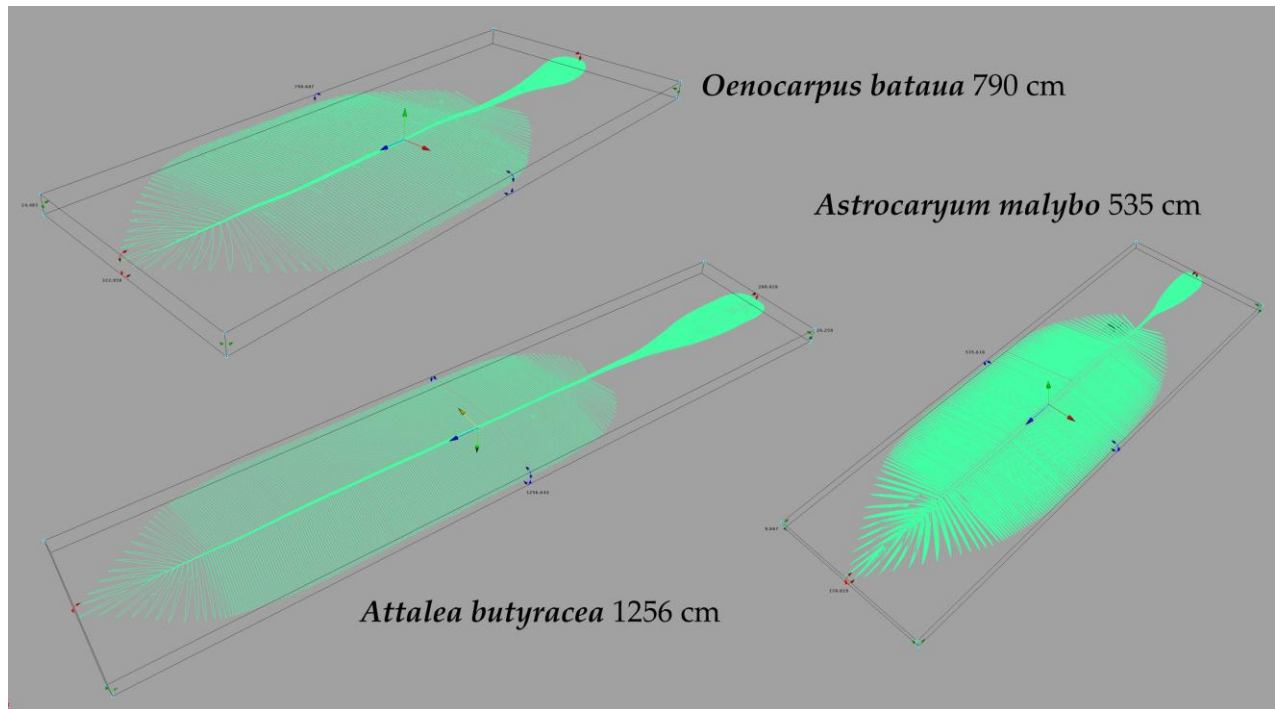


**Figure 13a.** Palm species modeling process results in the Maya 2009 software (Autodesk, 2008). Measures of the models in centimeters (review process of field measurements) are observed.

**Figure 13b (continued).** Palm species modeling process results in the Maya 2009 software (Autodesk, 2008). Measures models in centimeters (review process of field measurements) are observed.

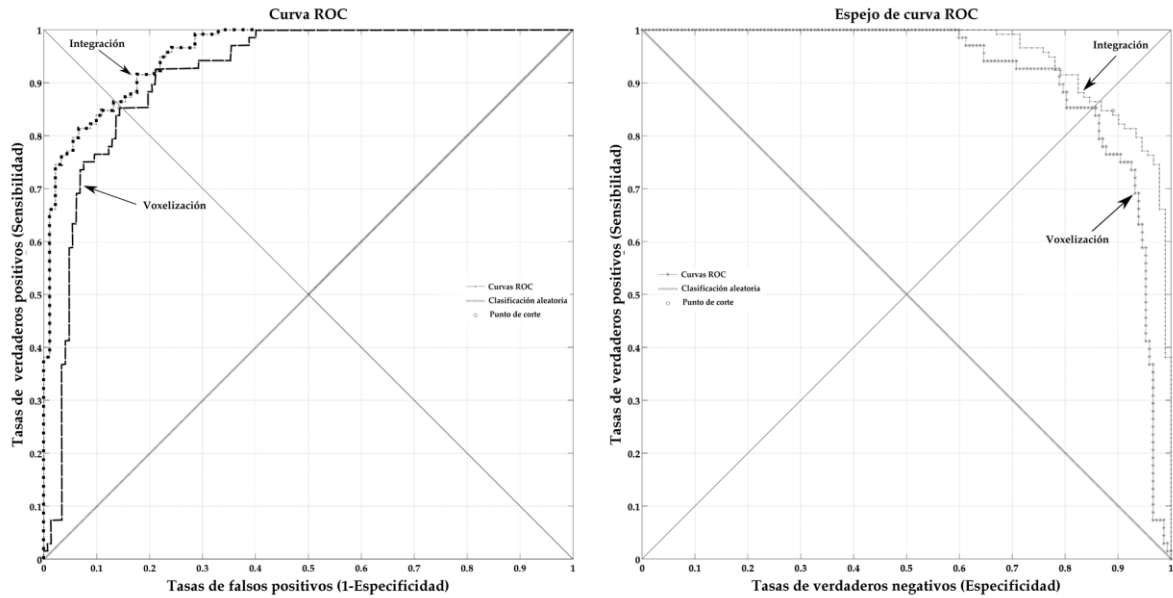


**Figure 14.** Rates of false positives and true negatives regarding the rates for the resultant true positives for the voxelisation and numerical integration methodologies. For the preparation of the figure the software MATLAB 2011b was used.

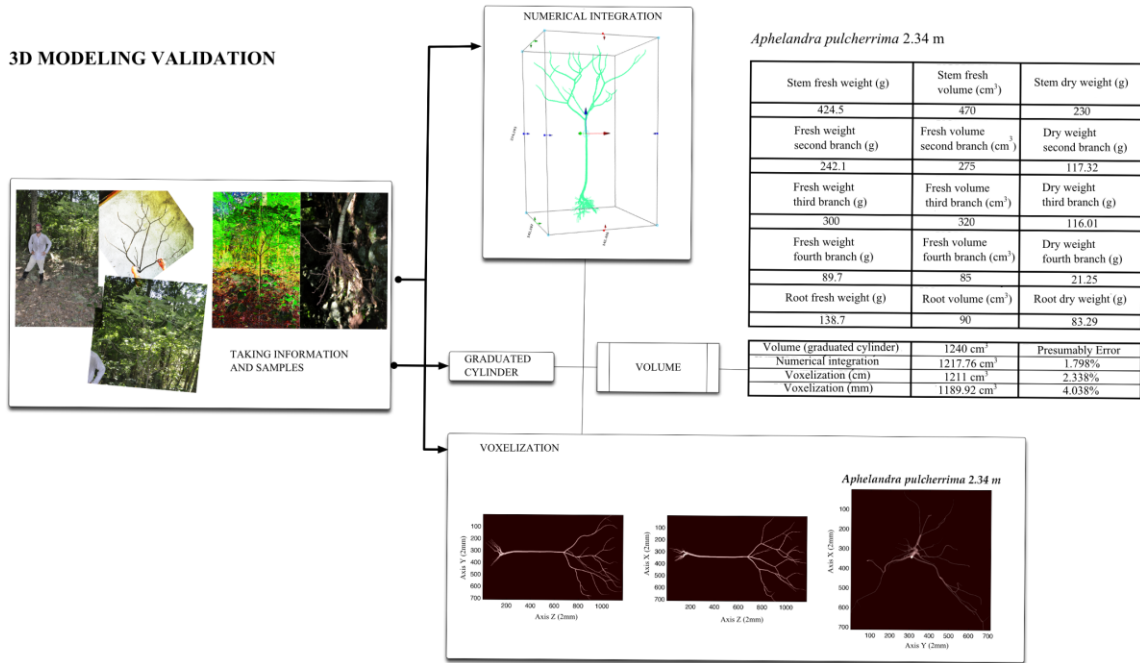


**Figure 15.** Voxelisation method validation process. For the preparation of the figure the software MATLAB 2011b and GIMP 2.6 was used.